ABSTRACT

Title of Document: CHARACTERIZATION OF TRACE METAL LEACHING FROM MARYLAND COAL FLY ASHES

Enes Ozkok, Master of Science, 2011

Directed By: Associate Professor Ahmet Aydilek, Department of Civil and Environmental Engineering

Three coal fly ashes with different acid-base characteristics and their mixtures with an embankment soil were analyzed for arsenic, copper, and chromium leaching as function of pH using batch-type water leach tests (pH 4−10). Leach tests results showed that significant Cu release occurred only at pH ~4.3 and dissolved Cr concentrations typically increased with increasing pH. Cr^{VI} was determined as the predominant oxidation state in leachates and results from WLTs spiked with Cr^{VI} suggest that Cr was strongly sorbed below pH 7. Sorption affinity of fly ashes for Cr^{VI} seemed to be to correlated to their oxalate-extractable Fe content, which is presumably a surrogate for amorphous iron (hydr)oxide content. Arsenic release typically followed a similar leaching pattern observed for Cr, with the exception of 100% alkaline fly ash; decreased As release above pH 9 for this sample was attributed to precipitation of Ca-As phases due to its high CaO content.

CHARACTERIZATION OF TRACE METAL LEACHING FROM MARYLAND COAL FLY ASHES

By

Enes Ozkok

Thesis submitted to the Faculty of the Graduate School of the
University of Maryland, College Park, in partial fulfillment
of the requirements for the degree of
Master of Science
2010

Advisory Committee:
Professor Ahmet H. Aydilek, Advisor, Chair
Professor Allen P. Davis, Advisor
Professor Alba Torrents, Committee Member

ACKNOWLEDGEMENT

First and foremost, I would like to thank my advisors, Professor Ahmet H. Aydilek and Professor Allen P. Davis for their guidance and patience throughout my graduate study at the University of Maryland College Park. Also a special thank is owed to my committee member Professor Alba Torrents for her support. Furthermore, I am very grateful to all of the faculty and staff members of Department of Civil and Environmental Engineering for their professionalism and resourcefulness.

Lastly, thanks to my beloved family for their support and my fellow labmates for their cheerful companionship during long work days in laboratory.

TABLE OF CONTENTS

LIST OF TABLES

LIST OF FIGURES

1. INTRODUCTION

Coal is the most abundant fossil fuel in the world, and unlike natural gas or petroleum, its reserves are more widely distributed (Twardowska and Stefaniak 2006, BP 2011). Accordingly, coal is mined and consumed as the primary fossil fuel in electricity generation industry worldwide; it is also an essential fuel for steel and cement production, and other industrial activities (WCI 2009). The biggest proven coal reserves are found in the United States (BP 2011), and hence approximately a billion metric tons of coal are annually combusted as a cheaper and more reliable domestic fuel source for electricity generation. In 2009, the net total electricity generation in the United States was 3,950 billion kWh and nearly 45% of the electric power was generated in coal-fired power plants (EIA 2011). Beside of its reliability, coal burning practices produce high amounts of solid residual and air-pollutant emissions.

Burning coal for electricity generation produces mainly mercury, CO_2, SO_2, and NO_X emissions, and understandably higher amounts of solid residuals (i.e., coal ash) compared to burning other types of fossil fuels. Different types of solid residuals are produced at large volumes as result of coal combustion and they are all commonly referred as *coal combustion products* (CCPs) instead of solely as "waste" to emphasize the possibility of beneficial reuse. CCPs include fly ash, bottom ash, boiler slag, flue gas desulfurization materials and other non-combustible solids in feed coal; the majority of CCPs consist of fly ash. According to the American Coal Ash Association's (ACAA) survey, 114 million metric tons of CCPs were produced in 2009 and 50% (57 million metric tons) of the CCPs produced in 2009 was fly ash (AACA 2011).

Fly ash forms the majority of CCPs produced at modern coal-fired power plants, making fly ash one of the most plentiful of the industrial by-products (PPRP 2008). Approximately 80-85% of the ash formed during combustion is entrained by exhaust gases and extracted by mechanical and electrostatic precipitators to control particulate matter pollution (Lindon 2001). This fine (silt-sized) particulate material separated from flue gas is called fly ash and the rest of the ash remaining at the bottom of boiler is called "bottom ash" (Keefer and Sajwan 1993). Fly ashes have pozzolanic properties due to their high content of silica, and metal oxides (Bin-Shafique, et al. 2006) Because of that, they can be reused in engineering applications, such as concrete production, road base and subgrade stabilization, embankments, and flowable fill (Ahmaruzzaman 2010). Additionally, depending on its chemical composition, fly ash can be used as a soil amendment due to its rich content of micronutrients (USEPA 2007).

The properties of fly ash can vary largely from source to source and over time. The physical, chemical and mineralogical properties of fly ash are strongly dependent on the properties of the feed coal, combustion conditions, type of pollution control facilities and handling (Baba et al. 2010, Komonweeraket 2010). During combustion, the temperature inside the boiler reaches above the melting point of most elements present in coal, and the components of feed coal undergo various chemical/physical changes and are redistributed (USGS 2002). The molten minerals cool as they are entrained by flue gases and form mostly spherical glassy fly ash particles (Dudas and Warren 1987, Lindon 2001). The organic content of the feed coal is combusted and removed depending on the efficiency of the combustion conditions (Hower et al. 1998). The incombustible inorganic content of feed coal is transferred to ash, hence coal ash exhibits much higher trace element

concentrations as a result of massive volume reduction (Keefer and Sajwan 1993, Baba and Kaya 2004).

According to ASTM C618, fly ashes are classified into two classes, Class C and Class F, based on the chemical composition and physical properties of the fly ash. Class C is produced from burning lignite and sub-bituminous coals that contain a high quantity of calcium carbonate ($CaCO_3$), resulting in an abundance of calcium oxide (CaO). Class F ash is derived from burning bituminous and anthracite coals that contain lower concentrations of calcium compounds. The hydration products produced from Class F fly ash possess little or no self-cementing characteristics and they often need to be activated with a cementitous agent for use in geotechnical applications (Yoon et al. 2009, Çetin et al. 2012).

Beneficial reuse of fly ash is crucial for sustainable management of CCPs. From 2003 to 2009, only 40 to 45% of fly ash was reused in various applications in the U.S. (AACA 2011). The fly ash that is not or cannot be reused is usually disposed in landfills or in ponds, and take up large volumes of space (Ahmaruzzaman 2010). The most common beneficial reuse for fly ash is to utilize it as a concrete additive; 40% of the fly ash in 2009 was beneficially reused by that way (AACA 2011). Fly ash produced in power plants located in Maryland and the Eastern U.S. used to be generally Class F, as a result of burning predominantly bituminous coal from the Eastern U.S. (PPRP 2008). Class F fly ashes can be reused as a concrete additive or in cement production (Çetin 2009). However, after the second phase of Title IV in the Clean Air Act Amendments of 1990 that were promulgated in 2000, and the resulting conversation to low-NO_X combustion, the combustion temperatures has been reduced. As a result, the carbon content of fly

ashes has generally increased all around the U.S. due to decreased combustion efficiency (Hower, et al. 1998). Fly ashes with high carbon content (>6%) cannot be used as a concrete additive due to interactions between carbon and air entrainment agents (Hill et al. 1997, Gao et al. 2002). This kind of fly ash, which is called "high carbon fly ash" (HCFA), is typically categorized as an "off-spec" fly ash, meaning that they do not meet the physical and chemical requirements criteria outlined in ASTM C618 and are therefore landfilled at large percentages (Çetin et al. 2012).

Nevertheless, HCFAs have a potential of being beneficially used in other applications, such as replacing natural materials in geotechnical applications, such as road base and highway embankment construction, instead of simply being landfilled (Ahmaruzzaman 2010). But before beneficially reusing fly ash in any type of land application, the environmental impacts should be thoroughly assessed. The most important drawback of reusing fly ash is its high trace metal content, which is subject to leaching, relative to the background soils (Bin-Shafique, et al 2002). Thus, metals leaching from fly ash-amended materials have the potential to contaminate nearby water bodies. Therefore, the leaching potential of HCFA should be evaluated by appropriate methods before any environmental decision-making. In this manner, the broader goal of this study is to assist in developing more appropriate test procedures for using fly ash (especially HCFA) in highway construction.

To accomplish this task, first the leaching characteristics of HCFAs should be well defined. But there is lack of research on the leaching potential of HCFA and HCFA/Soil mixtures, other than a limited number of studies (Bin-Shafique et al. 2002, Becker et al. 2010, Çetin et al. 2010, Komonweeraket 2010, Çetin et al. 2012). Thus, this study was

conducted to provide further information to fill gap in this field and focused on investigating leaching characteristics of fly ashes produced in the State of Maryland and their possible use in highway construction. Fly ash samples from three Maryland coal-fired power plants with the highest electricity generation capacities (PPRP 2008) and soil, which is a common borrow material for embankment construction in Maryland, were collected and were utilized to prepare mixtures.

The main object is to identify the chemical traits controlling the leaching of three trace metals (Arsenic, copper and chromium), by examining factors such as chemical composition of fly ash, pH of the solution and speciation of the metals. These three metals are selected primarily because of their high toxicity for aquatic life. Although the leaching behavior of metals from fly ash is dependent on many factors, solution pH is a the master variable controlling the leaching behavior of trace metals (Querol, et al. 1996, Kosson, et al. 2002, Bin-Shafique et al. 2006, Jegadessan et al. 2008, Jo et al. 2008, Baba et al. 2010, Komonweeraket 2010, Izquierdoa and Querol 2011) Therefore, to better investigate the impact of pH on leaching at numerous different pH values, batch-type leaching tests were conducted using mixtures, which were containing fly ash and soil at different percentages by weight, and leachates were analyzed for leaching characterization. The batch-type water leaching tests were preferred, because the leaching mechanisms are controlled by fewer variables and are easier to define (Kosson et al. 2002).

The work is presented in the following chapters. Chapter 2 outlines the materials used in this study and the procedures followed in performing the water leach tests and the other analyses. In Chapter 3, the results from the leaching tests at different pH values within

the range of 4-10 were given along with other supporting data to characterize the leaching behavior of arsenic, copper and chromium, and the mechanisms controlling the release of these elements were discussed in detail. Finally, in Chapter 4, the main conclusions of this study were provided.

2. MATERIALS AND METHODS

2.1. Materials

All fly ash and soil samples, which were utilized in preparing the soil-fly ash mixtures, were collected in the State of Maryland. Soil, which is commonly used in embankment construction by the Maryland State Highway Administration, was collected from a pit in Denton, Maryland and shipped to laboratory in 2010. Soil was crushed and dried in oven at 105°C for 24 hours before tests. Fly ashes were sampled from three Maryland coal-fired power plants with highest generation capacities in 2009. The fly ashes were labeled according to their sources; Brandon Shores (BS), Chalk Point (CP) and Morgantown (MT). The fly ashes were collected from power plants in dry form; hence fly ashes were not oven dried prior to tests.

The soil was classified as poorly graded sand with silt (SP-SM) according to the Unified Soil Classification System, and A-3 (fine sand) according to the American Association of State Highway and Transportation Officials (AASHTO) Classification System (Çetin 2010). Specific gravity of soil was determined as 2.6 (ASTM D 854) and its maximum dry density was 122 lbs/ft^3 at the moisture content of 11% (ASTM D 698).

BS fly ash was classified as Class F fly ash per ASTM C618 according to its X-ray fluorescence spectroscopy analyses (SiO_2+Al_2O_3+Fe_2O_3 Content =75%; CaO Content =1.1%) (Çetin 2010) and low loss on ignition, LOI (4.4%) (ASTM D 7848). CP and MT were classified as off-spec fly ashes due to their unburned carbon contents (i.e., LOI>6). The specific gravity of BS, CP and MT fly ashes were determined as 2.3, 2.2, and 2.4

(ASTM D 854), respectively. The properties of the three fly ashes and soil were summarized in Table 1.

Total elemental analyses (TEA) were performed on soil and three fly ashes according to the procedures outlined in EPA SW-846 Method 6800 by using a Thermo Jarrell Ash IRIS Advantage Inductively Coupled Plasma Optical Emission Spectrometer at the University of Wisconsin Soil Testing and Plant Analysis Laboratories and the results of the analyses summarized in Table 2.

2.2. Test Procedures

2.2.1. Compaction Tests

The fly ash and dry soil were homogeneously mixed at different proportions and tested for their maximum dry unit weight by using standard Proctor compaction effort (ASTM D 698). Before compaction tests, oven dried (105 °C) soil was sieved using a U.S. No. 4 sieve (4.76 mm). Because of relatively small particle size of the fly ashes, they were not sieved prior to compaction.

The mixtures were prepared with *x*% fly ash and (1-*x*)% sandy soil. Respective percentages of materials were based on their mass in the mixture (w/w). Additionally, some of the mixtures were prepared with two types of fly ash and sandy soil. If two types of fly ash were used to prepare the mixture, both type of fly ash were added at the same amount (both at *x*%) to the sandy soil ([1-2*x*]%). For example, 30 g BS were mixed with 70 g soil or 25 g BS and 25 g CP were mixed together with 50 g soil to prepare 100 g mixture. The fly ash and ssoil mixtures with a dry unit weight above 100 lb/ft^3 were

selected for further analysis. The list of mixtures and the results of compaction tests were given in Table 3.

2.2.2. Preparation of Fly Ashes and Soil Mixtures for Tests

Before sampling, soil was sieved through U.S. No. 10 sieve (2 mm) to adjust for the smaller size of the water leach testing equipment. Because of the small particle size of the fly ashes, they were sampled without sieving.

In the laboratory, soil, Morgantown fly ash (MT), Brandon Shores fly ash (BS) and Chalk Point fly ash (CP) were mixed as homogeneously as possible at different designated proportions. The percentages of the fly ash and sandy soil in mixtures were selected according to the preliminary compaction test (ASTM D 698) results. Each of the mixtures were stored inside capped containers and labeled. Additionally, some of the sandy soil and fly ashes were stored without mixing and labeled as 100% specimens.

2.2.3. Water Leach Test

Water leach tests (WLTs) were conducted with sandy soil-fly ash mixtures at different proportions. ASTM D3987 (*Standard Test Method for Shake Extraction of Solid Waste with Water*) was followed during leach tests with several modifications. The first modification was using 50-mL of total liquid volume instead of 2-L to fit the procedure to available laboratory equipment. The original liquid-to-solid ratio (S/L) of 1:20 g/mL (w/v) was not altered and was used for all samples throughout the study. The second modification was the usage of 0.02 M NaCl in deionized (DI) water instead of Type IV water to better simulate the ionic strength of the water percolating through upper soil cover above the compacted FA/Soil layer (Morar 2008, Becker 2010). Sodium chloride

was expected to have minimal effect on the leaching process. The last modification to the original ASTM D3987 procedure was adjusting final the pH of samples through the addition of either buffered solutions or HNO_3 to the extraction liquid.

WLTs were conducted with prepared mixtures that had desired compactability (>100 lb/ft^3) according to compaction test results. 2.50 g from each mixture was placed into 50-mL centrifuge tubes. Then, a volume of test water (0.02 M NaCl in DI water) equal in milliliters to 20 times the weight of mixture in grams was added into tubes. Tubes were capped carefully and placed onto the slot on the rotating arm of the tumbler. For each mixture, 3 replicates were prepared. Triplicate WLT samples for each were rotated continuously on a rotator (29 revolutions per minute) at room temperature (21 C^o - 23 C^o) for 18±0.25 hours. After the tumbling period, the WLT samples were centrifuged (2000 rpm, 10 minutes) and decanted into 60-mL plastic syringes. Suspended solids in the sample were filtered through 0.2-µm pore-sized 25-mm diameter membrane disk filters (PALL, Supor 200) fitted in a 25-mm Easy Pressure syringe filter holder. These extracted WLT samples were referred as the unbuffered leachates. Immediately after filtration, 10 mL of the aliquot from each leachate was allocated in a separate glass beaker and pH and electric conductivity were measured. The pH of extraction liquid was within the pH of range 5.3 to 5.7. The final leachate pH of samples varied greatly depending on the type of fly ash. The pH values of BS100, CP100, and MT100 leachates were 4.41, 6.56 and 9.88, respectively. The leachate pH of soil was 5.3. The rest of filtered samples were acidified to pH<2 using trace metal grade concentrated nitric acid (0.5% by volume) and stored in 50-mL high density polyethylene centrifuge tubes. All samples were stored at 4ºC for trace metal analysis.

Also WLTs with adjusted pH values were ran. The pH of the samples was fixed throughout the water leach tests by adding buffered solutions. The buffer solutions were prepared first by dissolving 0.1 M organic buffers provided from Sigma-Aldrich (MES, BES, EPPS, CAPSO and CAPS, >99%, anhydrous) in DI water. The organic buffers used in this study were assumed to have minimal interference with metals. Then, 1 M NaOH were added to the solutions until pH was fixed to the targeted value (pH 5.5, 7.0, 8.0, 9.0 and 10, respectively) within the effective pH range reported for the buffer type. After preliminary tests to determine the optimum volume of buffer solution for each mixture, buffer solutions were added to WLT test water (0.02 M NaCl in DI water) at the beginning of the leach tests.

To adjust the pH around 4 during WLTs, 1% (v/v) HNO_3 solutions were manually added to samples. The WLT samples were prepared with a total volume of 100-mL for this run (S:L=1:20 g/mL) to minimize the effect of volume change due to acid addition. The pH of the samples were checked every 15 minutes for the first 4 hours of the tests. Addition of 1% (v/v) HNO_3 solution were made to gradually adjust the pH around 4 by 0.1-ml addition at a time. When the pH of the samples were stabilized (around 4.3), the HNO_3 addition was stopped. However, the attempts of pH adjustment was failed for all of the MT-containing mixtures (i.e., MT100, MT60, MT50, MTBS25 and CPMT25) during the first 4 hours of WLTs, and the tests were terminated. Therefore, no data is available for these samples around pH 4.3.

2.2.4. Hexavalent Chromium Sorption Tests

To determine the sorption affinity of sandy soil for hexavalent chromium at different pH values, triplicate batch-type sorption tests were ran as *water leach tests* (WLTs) described

above with one exception. At the beginning of the adsorption tests samples were spiked either by 250 µg/L hexavalent chromium. Thus, the only difference between WLTs and sorption tests was the additional dissolved hexavalent chromium concentration in the extraction liquid.

For hexavalent chromium sorption tests, approximately 250 µg/L (±2%) of Cr^{VI} in 0.02 M NaCl was added to buffered and unbuffered WLT samples with 2.5 g of 100% soil and three kinds of fly ashes (S:L = 1:20 g/mL). As Cr^{VI} source, diluted 1000-mg/L chromate stock solution (Ricca Chemical, potassium chromate in DI water) were used. All samples were continuously tumbled for 18±0.25 hours at 29 rpm. After tumbling, the samples were centrifuged and filtered through the 0.2-µm pore-sized membrane filters. After the filtration, hexavalent chromium analysis was conducted with all leachates to determine the residual dissolved hexavalent chromium concentration. The remaining filtered leachates were acidified and stored at 4ºC until analyzed for total Cr by Atomic Adsorption Spectrometer (AAS).

2.2.5. Ammonium Oxalate Extraction

To estimate the total amount of As, Ca, Cr, Cu and P associated with amorphous Fe oxides and the dissolved Fe concentration as a surrogate of amorphous Fe oxides, a modified version of oxalate extraction method presented by McKeague and Day (1966) was utilized to selectively dissolve the amorphous fraction of Fe (hydr)oxides . 100 ml of 0.275 M acid ammonium oxalate (0.175 M Ammonium Oxalate + 0.1 M Oxalic Acid) solution was used as extraction liquid, adjusted to pH 3.0 ± 0.1 with 1 M HCl, transferred to glass beakers containing 2.5 g of different solid aliquots and a 1:40 solid-to-liquid (S:L=1:40 g/mL) ratio. Samples were mixed continuously by magnetic stirrers for 2

hours in the dark to minimize the possible photo-reduction of Fe^{III} in crystalline iron oxides, centrifuged for 10 minutes at 2000 rpm, and filtered through a 0.2-μm membrane filter. This filtrate was then collected in 50-mL centrifuge tubes and stored at 4°C until they were analyzed atomic adsorption spectrophometricly for As, Cr, Cu, Fe and colorimetrically for phosphate.

2.3. Analytical Techniques

All standards prepared for different analysis were prepared in an identical matrix to the samples. All calibration curves plotted were within the range where correlation between relationship between instrumental respond and the concentration was linear, and all samples were diluted accordingly to fit the concentration within the target range. Only calibration curves with coefficient of determination (R^2) of 0.995 or higher were accepted prior to analyses.

During measurements using atomic adsorption spectrophotometry (AAS), duplicate measurements were made from each sample. If the relative standard deviation (RSD) between 2 replicate readings from the same sample was below 5%, the reading was accepted as correct and the arithmetic average of the two reading from same sample was recorded as the actual metal concentration of the sample. For each run, a calculated-intercept type calibration curve was fitted automatically by the software (AA Winlab^{TM}) to analysis results of standards and blanks, which were prepared identical to the matrix of the samples being analyzed. Calibration of the instrument is checked after measurement of 10 samples by analyzing 2 of the standards prepared for calibration. If the reading was within the ±5 percent of the standards' concentration, the analyses continued. If

calibration check is failed, blank standard was checked. If the blank was very close to calculated intercept (±10%), 2 of the standards were checked again. If the calibration check failed second time or blank reading changed over 10% , the instrument was recalibrated.

2.3.1. Electrical Conductivity Measurements

The conductance of the leachates was measured with YSI Model 35 Conductance Meter, immediately after the samples filtered through 0.2 µm membrane filters. The tip of the probe was repeatedly submerged a minimum of three times into the solution being tested to allow the conductance meter to stabilize. Once the same conductance value was measured three times successively, it was recorded. Again, thorough rinsing of the probe was carried out to prevent contamination. The conductance readings in mS (millisiemens) units were corrected for temperature and then converted to electrical conductivity (EC) in µS cm^{-1} units at 25°C .

2.3.2. pH and ORP Measurements

All WLT and batch-type adsorption test samples were analyzed for pH immediately after filtration (0.2 µm membrane filter) by using Orion Model 520A pH meter installed with a pH probe (Orion, Model 91560), before acidification. Before measurements and every 4 hours during measurements, the pH meter was calibrated with 3 buffer solutions at pH 4.00, 7.01 and 10.01. The probe tip was thoroughly rinsed with deionized water between each standard and sample measured.

Oxidation reduction potential (ORP) measurements were conducted only on WLT samples without pH adjustments by Orion Model 520A pH meter installed with a ORP

probe, immediately after centrifuge. The redox potentials (E_h) of leachates were reported in unit of milivolts (mV).

2.3.3. Dissolved Chromium and Copper Analyses

The total dissolved chromium and copper concentrations in the leachates were determined by using graphite furnace atomic adsorption spectrophotometry according to standards published by APHA (1995). 1 mL from acidified triplicate WLT samples in plastic tubes were placed to auto-sampler slots and duplicate readings were conducted for each sample. Copper standards and Chromium standards were ranged from 0.5 to 50 ppb. The detection limit of this method for Cu and Cr was determined as 0.4 and 0.6 µg/L, respectively, according to EPA's standard method 1030E.

2.3.4. Dissolved Iron and Calcium Analyses

Iron concentration in oxalate extracts was measured by AAS Flame Technique. Compressed air was used as gas and acetylene is used as fuel. Standards which have same matrix with samples were prepared containing Fe form 0.05 to 5 mg/L. There were 1 mL oxalate extraction liquid in 50 mL and 0.25 mL concentrated HNO_3 in standards. Samples were also diluted 20 or 50 times and 0.25 mL nitric acid was added to drop the pH below 2. The method detection limit (MDL) for Fe was determined as 0.03 mg/L according to EPA standard method 1030E.

Calcium in the unbuffered WLT leachates was measured by AAS Flame Technique. NO_2 was used as gas and acetylene was used as fuel. Standards which have same matrix with samples were prepared containing Ca form 0.05 to 5 mg/L. The method detection limit (MDL) for Ca was determined as 0.05 mg/L according to EPA standard method 1030E.

2.3.5. Dissolved Arsenic Analyses

The total dissolved arsenic concentrations in the leachates were determined by using Perkin Elmer 5100 ZL atomic adsorption spectrophotometer, with an electrodeless discharge lamp (EDL) as the radiation source. Due to low arsenic concentrations at µg/L levels, continuous hydride generation technique (APHA 1995) was followed with the modifications recommended by the manufacturer instrument.

0.5% $NaBH_4$ in 0.05% NaOH was used as reductant and 10% (v/v) HCl solution was used as carrier liquid during analysis. 3 mL from WLT extracts were transferred to 15-ml plastic centrifuge tubes. Then 3 ml reducing agent, which was prepared by dissolving 10% (w/v) potassium iodide and 5% (w/v) ascorbic acid in DI water, and 3 mL trace metal grade concentrated HCl were added to the extracts and let stand for at least 45 minutes. Finally, the resulting test solutions were diluted again with 3-mL of 10% (v/v) HCl solution before analysis.

The test solution was pumped into a stoppered separatory funnel which was used as the reaction vessel. During analyses, daily prepared reductant and 10% HCl was continuously injected into the reaction vessel at the flow rate of 5-6 and 9-11 mL/min, respectively. The released H_3As was transported through tubing by a 50-100 mL/min Ar gas stream to a quartz cell centered on the optical beam of the spectrometer. The cylindrical quartz cell was heated electrically up to 900 °C. The As atomized in the heated quartz cell was measured with 193.7 nm radiation. The absorbance peak area integrated over 15 s was used as the analytical signal. For calibration, the arsenic standards from 0.5 to 50 µg As/L were prepared and only calibration curves with

$R^2 \geq 0.995$ were accepted. The arsenic detection limit of this technique was determined as 0.4 µg/L according to EPA standard method 1030E.

2.3.6. Hexavalent Chromium Analyses

Hexavalent chromium, Cr^{VI}, in the leachates was determined by using the spectrophotometric method described in the paper by Bartlett and James (1979) with minor modifications. 1 mL of *s*-diphenyl carbazide reagent was added to 8 mL of leachate aliquot. All specimens (reagent-leachate mixtures) were mixed vigorously and allowed to stand 20 minutes. After 20 minutes, the intensity of magenta color developed in each specimen was measured by spectrophotometer (UV-Visible Recording Spectrophotometer, Shimadzu UV160U) at wavelength of 540 nm using cuvette with a light path of 1.0 cm.

The instrument was calibrated for each batch of measurements by a set of standards which were prepared at the same time with other specimens, because the reagent's color development characteristics changes over time. The *s*-diphenyl carbazide reagent (Ricca Chemical Company, ACS Grade) was prepared by adding 120 mL of 85% H_3PO_4, diluted with 280 mL of deionized water, to 0.2 g of *s*-diphenyl carbazide dissolved in 100 mL of 95% ethanol.

A set of at least 6 standards plus blank were prepared each time freshly from 1000 mg/L Cr^{VI} stock solution (Ricca Chemical, potassium chromate in DI water) to eliminate any possible alteration in concentration due to chromium reduction in the diluted standards during storage. First, the stock solution was diluted to 1 mg/L (1000 µg/L, or ppb) and then the standards with concentrations ranged from 10 to 500 µg/L were diluted from this

1-mg/L intermediate solution. Calibration curves were linear within this range ($R^2 \geq 0.999$). All dilutions for standards and the blank were prepared using 0.02 M NaCl in deionized water to obtain a matrix similar to the leachates. MDL for these analyses accepted as the lowest standard (10 µg/L). When the Cr^{VI} concentration was below 10 µg/L, the T value was ≤1%.

2.3.7. Phosphate Analyses

Dissolved phosphate concentration in the oxalate extracts was analyzed using the method of Wolf and Baker (1990). This method calls for the use of 0.275 M acid ammonium oxalate solution and therefore, the oxalate extraction method was modified accordingly in this work. After filtration through a 0.2-µm membrane filter, samples were analyzed colorimetrically for phosphate at 880 nm. 5 standards ranging from 50 to 500 µg/L plus 1 blank were prepared for plotting the calibration curve. The relationship between phosphate concentration and corresponding absorbance was linear within this range and coefficient of determination (R^2) for the plotted calibration curve was higher than 0.995.

Dissolved phosphate in WLT extracts were analyzed as described by Pote and Daniel (2009). Blank plus at least 6 standards prepared ranging from 10 to 500 µg/L in 0.02 M NaCl ($R^2 \geq 0.995$). Samples were analyzed colorimetrically for phosphate at 880 nm using cuvette with a light path of 1.0 cm.

3. RESULTS AND DISCUSSION

3.1. The Natural pH of the Leachates

The geometric averages of pH measurements from triplicate WLTs without pH adjustment are summarized in Table 4. These listed pH values are accepted as the natural pH values of the leachates from soil, fly ashes (FA) and FA/soil mixtures in contact with identical extraction liquid without any buffer solution or HNO_3 addition (0.02 M NaCl in DI water with pH ranging from 5.3 to 5.7). The leachate from pure soil (SOIL) had a pH of 5.32. The pH of the leachates from 100% CP, BS and MT were 4.41, 6.53 and 9.83, respectively. Natural pH values of leachates from FA/Soil mixtures were typically between those for the soil and the particular fly ash alone, but pH tended to be closer to that obtained from respective type of 100% fly ash sample. Therefore, it appears that the great variation between the final H^+ activities of the leachates ($10^{5.4}$ times) was originated from the combined effect of alkaline and acidic components of the soil and especially of fly ashes in the mixtures.

The highest pH values belonged to leachates from MT100 and MT/Soil mixtures (i.e., MT40, MT50, MT60) and pH of leachates increased from 9.50 to 9.83 with the increasing MT content (from 40% to 100%). Alkaline characteristics of MT-containing samples can be explained by significantly higher Ca leaching from these mixtures (46−90 mg/L) compared to other 100% FA and FA/Soil mixtures (4.7−30 mg/L) (Table 4) , since the primary mode of occurrence of Ca in fly ash is CaO (USGS 2002). Alkalinity of fly ash leachates is mainly associated with hydrolysis of CaO in the solid phase upon exposure to water (Talbot et al. 1978, Dudas 1981, Dudas and Warren 1987, Nathana et

al. 1999, Kim 2006, Gitari et al. 2008, Ward et al. 2009,) and the reactions generating alkalinity can be expressed as (Equations 1 and 2):

$$CaO + H_2O \rightarrow Ca(OH)_2 \qquad \text{(Hydrolysis of lime)} \qquad (1)$$

$$Ca(OH)_2 \rightarrow Ca^{2+} + 2\,OH^- \qquad \text{(Dissolution of calcium)} \qquad (2)$$

As seen above, hydrolysis of 1 mole of CaO can produces 2 moles of alkalinity and 1 mol of dissolved Ca ion. Therefore, dissolved Ca concentration in the leachate can be used as a surrogate for dissolved fraction of CaO content released into the aqueous phase from solid fly ash matrix. Likewise, dissolution of other alkaline and earth alkaline oxides in fly ashes (e.g., MgO, K_2O and Na_2O) can also contribute to alkalinity formation in the leachate. However, potassium and sodium oxides are less readily soluble (Talbot et al. 1978, Dudas 1981) and the total Ca content of all FAs were significantly higher than respective total Mg content.

According to TEA data (Table 2), total Ca content of MT, CP and BS was 10100, 3300 and 2200 mg/kg, respectively; total Mg content of MT, CP and BS was 5800, 1500 and 1000 mg/kg, respectively. Strong correlation (R^2=0.93) between dissolved Ca concentration and the electrical conductivity (EC), which is an indicator for the total amount of dissolved solids in the solution (Sparks 2003), implies that dissolved Ca is a major constituent of the leachate and/or other soluble major species were also dissolved and present in the leachate at an extent similar to Ca for each sample (Figure 1) (Simòn and Garcìa 1999). Kim (2006) reported that using solely dissolved Ca concentration or using dissolved Ca and Mg concentration together makes no significant change in strength of the linear correlation between alkalinity and dissolved elements for 35 Class F

fly ashes leachates. Furthermore, the relationship between dissolved calcium content and alkalinity is also supported by the failed attempts of pH fixation around 4.3 for MT-containing mixtures, suggesting strong acid neutralization capacity of these samples.

When dissolved Ca concentrations from WLTs without pH adjustment were plotted against corresponding leachate pH values, it appears that pH did not always increase as dissolved calcium content in leachate increased (Figure 2). The leachate from CP100 had the second highest dissolved Ca concentration (30 mg/L) following MT-containing mixtures. However, increased CP content caused a decline in the leachate pH values; leachate pH values for CP30, CP40 and CP100 were 5.32, 4.34 and 4.41, respectively. It appears that CP had high acidity-forming capability that overwhelmed the effect of its dissolved Ca content in the solution.

In Table 5, dissolved Fe concentration from oxalate extraction tests are given, along with percentage of oxalate-extractable iron content relative to total iron content of the materials. Acidic ammonium oxalate solution (pH=3) can selectively extract amorphous and poorly crystalline iron oxides (McKeague and Day 1966). All extracted iron was attributed to amorphous iron (hydr)oxide. According to the results, CP had the highest oxalate-extractable iron concentration (10600 mg/kg), implying that 40% of total iron was in form of amorphous iron oxide (Table 5). MT fly ash had a total Fe content comparable to CP, but only 21% of it was oxalate-extractable. BS fly ash had the lowest total Fe content (approximately 25% of other fly ashes) and 27% of it was oxalate extractable iron. Dudas (1981) observed formation of amorphous iron oxide as secondary minerals during weathering of fly ash. A more soluble portion of the iron from reactive glassy surfaces of fly ash particles can precipitate as amorphous iron oxides during the

weathering process (Theis and Wirth 1977, Dudas and Warren 1987) and form acidity analogous to precipitation of free iron and aluminum in soil solution (Sparks 2003, Sposito 2008) (Equation 3).

$$Fe^{3+} + H_2O \rightarrow Fe(OH)_{3(s)} + 3\ H^+ \qquad \text{(Precipitation of free Fe ion)} \qquad (3)$$

As seen above, each mole of Fe^{3+} ion generates three moles of hydrogen ion as a result of precipitation.

Amorphous Al oxides can also be extracted by ammonium oxalate solution(McKeague and Day 1966); however Al was not detected above the MDL of 5 mg/L (200 mg/kg per solid) in the extracts, despite total Al content of fly ashes ranging from 21300 to 26300 mg/L. It appears that virtually all of the Al in fly ash and soil was found in less reactive crystalline structures and did not form amorphous Al oxides (Dudas and Warren 1987, Apul et al. 2005).

Therefore, oxalate-extractable Fe concentrations can be used as a surrogate for precipitated amorphous iron oxides to predict the acidic character of CP and other fly ashes. Oxalate-extractable Fe content for each mixture is estimated based on linear dilution calculations using the oxalate-extractable Fe content of pure materials listed in Table 5 (Equation 4).

$$Fe_{ox} = \sum_{i=1}^{n} (f_i \times C_i) \qquad (4)$$

where Fe_{ox} is the oxalate-extractable Fe content of the mixture (mg/kg); f_i is fraction of *i*th material in the mixture; and C_i is the oxalate-extractable Fe content of *i*th material in the mixture (mg/kg). Additionally, the dissolved Ca concentrations (mg/L) are converted

to Ca concentration per kg solid (S:L=1:20 g/mL). Estimated values for the two parameters are listed in Table 4. In order to better investigate the relation between leachate pH and chemical composition, three additional mixtures (BS40, CP40 and MT40), which were not analyzed for trace metals, were prepared and analyzed for dissolved Ca concentration (Table 4).

Assuming the major components affecting pH are dissolved Ca and amorphous iron content, the relationship between these metrics and pH can be described using the dimensionless ratio of dissolved Ca content (mg/kg) over oxalate-extractable Fe content (mg/kg) (Table 4). Figure 3 shows that calculated ratios for each mixture correlates well with leachate pH (R^2 =0.84) and presents a delineation of acidic or basic character of fly ashes from pH 4.34 to 9.83. However, the difference between two values were 4 orders of magnitude, suggesting that only a very small portion of oxalate-extractable Fe content actually precipitate as secondary mineral and contribute to pH formation.

Since WLTs are batch-type tests, the soluble Ca content and acid-forming content were in equilibrium and form the natural pH of the leachates. However, constituents of FA/Soil mixtures may be weathered under field conditions and the highly aqueous-soluble components, such as calcium, can be washed away over time (Dudas 1981, Talbot et al. 1978, Ward et al. 2009). Correspondingly, pH of the FA/Soil layer solution can change, or initial pH of the percolating water can affect final leachate pH. Therefore, testing the leaching character of the mixtures as a function of pH can provide valuable information on possible long-term leaching risks.

3.2. Overall Leaching Trend as a Function of pH

The results of water leach tests (WLTs), which were conducted under pH-controlled conditions, are summarized in Table 6; the mean pH, electrical conductivity (EC) and arsenic, copper and total chromium concentrations are tabulated together along with hexavalent chromium concentrations. The electrical conductivities and dissolved metal concentrations are reported as the arithmetic mean of the readings from triplicate samples, whereas pH values of the leachates are presented as the geometric averages.

The values of As, Cu and Cr concentrations given in Table 6 represent the total dissolved metal concentrations without differentiating between particular species of metals released into the aqueous phase (i.e., leachate). Hence, these metal concentrations measured in the leachates (filtered through 0.22-µm pore-sized membranes) are referred as total dissolved or leached metal concentrations, and are assumed to be completely mobile metal fractions as a result of partitioning-equilibrium between solid and liquid phases that are controlled by rather complex interactions at solid-liquid interfaces(Evans 1989, Stumm and Morgan 1996).

In order to better compare the leaching from different mixtures as a function of pH, the leached metal concentrations were normalized by total metal content of each mixture to minimize the impact of the difference in elemental concentrations. The total metal contents of each mixture were calculated using (Equation 5) and then the total dissolved metal mass per unit weight of solid material was calculated and divided by the calculated total metal content of the mixtures (Equation 6). The resulting ratio between dissolved and total content is referred as *the leachability* of a particular metal in water. Figure 4

shows the calculated metal leachability of analyzed trace metals. The maximum leachability values for pure materials are listed in Table 7.

$$TC = \sum_{i=1}^{n} (f_i \times C_i) \tag{5}$$

where TC is total metal content of the mixture (mg/kg); f_i is fraction of *i*th material in the mixture; and C_i is total metal concentration of *i*th material in the mixture (mg/kg).

$$Leachability = \frac{C_{Leached} \times V}{m \times TC} \tag{6}$$

where, C_{Leached} is dissolved metal concentration in the WLT leachate (mg/L); V is volume of leachate (0.050 L); m is mass of the mixture (0.0025 kg for WLTs).

The leaching is the release of the constituents in the solid material into the aqueous-phase through contact with water and governed by two main mechanism undergoing simultaneously, sorption and solubility (Evans 1989, van der Sloot et al. 2003). Both mechanisms are strongly depended on the pH of the solution (Evans 1989, Stumm and Morgan 1996). As seen in Figure 4, dissolved metal concentrations for 12 different mixtures demonstrates a strong dependency on leachate pH. Significantly high Cu leaching was observed only under strongly acidic leachate pH and significant As and Cr release was only exhibited under alkaline conditions.

The overall trend of trace metal leaching appears to be similar for all mixtures, although they were prepared using different materials at different proportions. However, the great variation between observed maximum leachability for each material under similar conditions suggests a significant impact of different chemical composition of each material. A fraction of the constituents may be trapped inside less reactive glassy fly ash

particles and may not leach into the aqueous solution at all (Dudas and Warren 1987), whereas some of the constituents may be more labile in the presence of water but their leachability as a function of pH is controlled by their mode of occurrence (Keefer and Sajwan 1993, Querol et al. 1996, Wang et al. 2008,). For example, Querol et al. (1996) reported that the elements associated with sulfates are more water extractable and the elements are embedded into aluminosilicate phases have lower mobility.

Briefly, the surface chemistry of FA/Soil mixtures is rather complex and depends on multiple factors. Thus conducting water leach tests at different pH values are crucial for each type of mixture because leachate pH depends on exact chemical composition of the mixture and linear dilution calculations do not predict the leaching behavior of trace metals (Çetin et al. 2012, Bin-Shafique 2006). For example, at their natural pH values, Cr release from MT50 (120 µg/L at pH 9.57) and MT60 (150 µg/L at pH 9.73) is almost 50% and 60% of the Cr leaching from MT100 (230 µg/L at pH 9.83), respectively (Table 6). A similar relationship between MT content of the sample and the dissolved Cr concentration was also available for WLT with pH values buffered to ~9.35 (Figure 5). However, when the pH of MT samples were fixed pH values below 9, the correlation became non-linear. A linear relationship between As leaching from MT-containing mixtures and the MT fly ash content was not available at all within the pH range of 6−10 (Table 6). Therefore, analyzing solely leaching potentials of pure materials as a function of pH is not adequate; the leaching potentials should also be analyzed for each specific kind of mixture.

3.3. Leaching Behavior of Chromium

Total dissolved chromium (TD Cr) and dissolved hexavalent chromium (Cr^{VI}) concentrations within the pH range of 6−10 for MT100 and MT/soil mixtures are plotted in Figure 6. Cr leaching from MT100 was 110 µg/L at pH 6.23 and significantly increased to 270 µg/L at pH 10.3. Similar to the trend observed for MT100 but to a lesser extent, MT/Soil (Figure 6), MTBS25 and CPMT25 (Figure 7) mixtures also exhibited monotonically increased Cr leaching with increasing pH. TD Cr concentrations from MT-containing samples other than MT100 ranged from 28 to 97 µg/L at pH ~6 and become 67−150 µg/L within the pH range of 9−10.

The average dissolved Cr^{VI}-to-TD Cr ratios listed in Table 6 for MT-containing mixtures are 110±15%, demonstrating that Cr leaching was predominantly in form of Cr^{VI} for these mixtures. Within the pH range of 4−10, dissolved Cr^{VI} is almost completely present in form of chromate species ($HCrO_4^-$ and CrO_4^{2-}) with negative valence (Figure 8); pK_{a1}=2.0 and pK_{a2}=6.5 (Stumm and Morgan 1996).

Under acidic to neutral pH ranges, the retention of oxyanion-forming trace elements (such as Cr^{VI}, As and Se) may be explained by sorption onto metal oxides, which are abundant components of Class F fly ashes (Keefer and Sajwan 1993), according to double diffuse layer (DDL) theory that is used to explain sorption in soil solution (Yu 1997, Sparks 2003). In the presence of water, metal oxides acquire surface hydroxyl groups protruding from the solid surface into the solution (Hohl et al. 1980, Stumm and Morgan 1996). These resulting surface hydroxyl groups can be protonated or

deprotonated depending on pH of the solution (Equation 7) and create variable charge on the surface of metal oxides (Hohl et al. 1980, Stumm and Morgan 1996):

$$\equiv Me{-}OH_2^+ \leftrightarrow \equiv Me{-}OH + H^+ \leftrightarrow \equiv Me{-}O^- + 2\,H^+ \quad (7)$$

where metal atoms on the surface that exhibit amphoteric behavior are designated by '≡Me'. The pH-dependent negative and positive surface charges are discrete, but not neutralized by each other (Yu 1997). The net surface charges become zero ($[\equiv Me{-}OH_2^+] = [\equiv Me{-}O^-]$) at some intermediate pH value, which is referred to as *the point of zero charge* (pH_{pzc}) (Stumm and Morgan 1996). At pH values lower than pH_{pzc}, a positive charged surface prevails and oxyanions electrostatically sorb onto the surface; when the pH of the solution becomes higher than pH_{pzc}, a predominantly negatively charged surface is formed and the sorption affinity for oxyanions diminishes (Yu 1997, Sparks 2003). Overall, the reversible sorption reaction for chromate species onto hydrated metal oxides can be simply expressed as below (Equations 8 and 9),

$$\equiv Me{-}OH^0 + CrO_4^{2-} + H^+ \leftrightarrow \equiv Me{-}OH_2^+ \text{---} CrO_4^{2-} \quad (8)$$

$$\equiv Me{-}OH^0 + HCrO_4^- + H^+ \leftrightarrow \equiv Me{-}OH_2^+ \text{---} HCrO_4^- \quad (9)$$

Where the dashed line ('---') stands for the bond due to electrostatic attraction between surface functional group and the chromate ions (Equations 8 and 9). The electrostatic attraction effect the mobility of oxyanions over a wide pH range for metal oxides with high pH_{pzc} (Stumm and Morgan 1996, Sparks 2003). Among different types of metal oxides, amorphous Al and Fe oxides are claimed to be the ones that most efficiently sorb oxyanions, such as Cr^{VI} and As^V, because of their large surface area, microporous structures, and abundance of binding sites (Coughlin and Stone 1995, Apul et al. 2005).

The reported pH_{pzc} values for amorphous ferric (hydr)oxide ranges from 7.9 to 8.5 (Hsia et al. 1993, Sparks 2003).

The same sorption mechanism may also apply for other non-MT-containing samples (BS100, BS/Soil (Figure 9), CP100, CP/Soil (Figure 10) and BSCP20 (Figure 7)), however Cr release from these mixtures is relatively very low over the pH range of 4−10 (≤37 µg/L) and the Cr^{VI}-to-TD Cr ratios can only be obtained for a few pH points (Table 6). Furthermore, WLT data from these mixtures were available below pH 6 and Cr concentrations follow a U-shaped pattern with increasing pH, due to Cr release at pH ~4.3 (≤19 µg/L) comparable to release at alkaline pH ranges. Therefore, in order to better compare the leaching characteristics of 3 types of fly ashes, sorption tests were conducted using BS100, CP100 and 100% soil samples. Sorption tests were completed as WLTs that were spiked with 250 µg/L chromate, since the Cr release from MT100 was predominantly in form of Cr^{VI} and the highest Cr concentrations detected were around 250 µg/L. The concentrations of residual Cr and Cr^{VI} for the spiked WLTs are listed in Table 8.

The residual Cr concentration measured in spiked sorption test samples and the inherent Cr release measured in WLTs are plotted together in Figure 11 for BS100 and in Figure 12 for CP100. Considering the different chemical compositions of the two types of fly ashes, the results of sorption tests as a function pH exhibit similar trends. From pH ~5.5 to ~7, the residual Cr concentrations obtain the lowest values, like inherent Cr release. For other mixtures containing only BS and CP, the Cr release was insignificant (<10 µg/L) between the pH range of 5.5 to 7 (Figure 7, Figure 9, Figure 10). From pH ~7 to ~9, the residual Cr concentrations sharply increased; from 160 µg/L at pH 7 to 320 µg/L

at pH 8.7 for BS100 (Figure 11); from 97 µg/L at pH 7 to 240 µg/ at pH 8.3 for CP100 (Figure 12). -Similarly to the increase in residual Cr concentration, inherent Cr leaching from all BS and CP-containing mixtures also increased as the pH increased further above 7. Increased Cr leaching from WLTs and spiked sorption test samples, suggesting that the sorption affinity of fly ash particles for chromate gradually decreased within the pH range of 7-9.

Above pH 9, the inherent Cr release from BS100 (Figure 11) and CP100 (Figure 12) increased almost parallel to the increase in residual Cr concentrations and the additional Cr^{VI} concentration (250 µg/L) began to be completely recovered, since the difference between inherent Cr release and residual Cr concentrations from BS100 and CP100 became higher than 250 µg/L. This observation can be interpreted as the depleted sorption capacity for additional Cr^{VI} above pH 9 due to predominately negatively charged surface and the Cr oxyanions repelled from the surface (Yu 1997). Additionally, these results can be interpreted as the absence of Cr reduction, because the spiked Cr^{VI} concentration was completely recovered according to both total dissolved Cr and dissolved Cr^{VI} analyses.

The available sorption test results for 100% FA and soil samples are roughly extrapolated to pH 6 to estimate the difference between inherent Cr leaching and residual Cr concentration. Then the estimated value is subtracted from the spiked Cr concentration of 250 µg/L and the resulting value is accepted as the sorbed portion of additional 250 µg/L chromate onto the surface FA of particles at pH 6. During the calculations, the total dissolved Cr concentrations were used, presuming that the AAS technique is more accurate. The total dissolved Cr-to-Cr^{VI} ratio is assumed as equal to 1 for these

calculations. For instance, the difference between inherent Cr leaching and residual Cr is estimated as ~175 µg/L for BS100. Thus the adsorbed Cr concentration is found to be around 70 µg/L, whereas d 175 µg/L is estimated for CP100. Stable trend in residual Cr concentration from BS100 at 5.6−7 suggests that the ~70 µg/L additional sorption capacity is the maximum level for BS100. The residual Cr concentration detected in spiked CP100 leachate was 8 µg/L at pH 4.3. Naturally leached Cr concentrations from CP100 were 4.0 µg/L at its natural pH of 4.41 and 13 µg/L at pH 4.27. It appears that CP can retain virtually all of the spiked chromate concentration of 250 µg/L at ~4.3.

The significant difference between sorption capacities of BS and CP can be attributed to their amorphous iron contents. The oxalate-extractable dissolved Fe concentration for BS and CP were 1700 and 10600 mg/kg, respectively (Table 5), suggesting that CP had approximately 6 times higher amorphous iron oxide content. Moreover, the sharp increase of residual Cr concentrations within a narrow pH range implies that the sorption of Cr^{VI} is controlled by single type of surface. This surface is presumed to be amorphous Fe oxide; the reported pH_{pzc} values for amorphous Fe oxide are within the pH range of 7−9, where the bulk of the sorption capacity for additional Cr^{VI} was almost depleted. Moreover, no oxalate-extractable Al was found above detection limit (200 mg/kg), suggesting negligible amounts of amorphous Al oxides, which is also claimed to be have significant effect on sorption, were present in the samples compared to amorphous Fe oxides.

The MT100 mixtures were also spiked with 250 µg/L chromate (Table 8). As seen in Figure 13, residual Cr concentration from spiked MT100 samples followed a highly fluctuating pattern but never increase significantly within the pH range of 6−9.8. The

sorbed portion of additional Cr^{VI} was calculated as 40 µg/L at pH ~6, which is lower than the sorption capacity for BS100 around pH 6, despite the considerably higher oxalate-extractable Fe content of 5300 mg/kg than BS100. However, additional sorption capacity of MT100, 80 µg/L at pH 8, 240 µg/L at pH 9.14, and 120 µg/L at pH 9.8, suggesting greater Cr^{VI} sorption capacity above pH 9, unlike observed sorption trends for BS100 and CP100. This was also confirmed by an additional sorption test conducted with 1000 µg/L Cr^{VI}. The residual Cr concentration in the leachate from MT100 spiked with 1000 µg/L of Cr^{VI} was measured as 860 at pH 9.14 (Table 8) and the sorption capacity for additional Cr^{VI} was calculated as 370 µg/L for this sample; it also demonstrated that there was no saturation for Cr^{VI} at least up to 860 µg/L at pH 9.14.

The sustained affinity for additional Cr^{VI} above pH 9 can be a result of reduced amount of P and As oxyanions competing with Cr^{VI} for sorption same sites on amorphous iron oxide surfaces (Zachara et al. 1987, Fruchter, et al. 1990). High concentrations of oxalate-extractable As (52 mg/kg) and P (100 mg/kg) were detected in MT100 (Table 9), but the dissolved concentration of both elements decrease above pH 9 (Table 6 and Table 10) as they were probably precipitated and removed from the solution. For example, from pH 9.4 to 9.8, the dissolved P concentration decreased from 110 to 89 µg/L (Figure 14). This ~24% of reduction corresponded to 420 mg/kg drop in dissolved P concentration and can create sorption sites that were available to Cr^{VI}, considering the total Cr content of 68 mg/kg for MT100. Zachara et al. (1987) reported that the presence of dissolved Ca in the solution increased Cr^{VI} sorption above pH 7, hence high dissolved Ca concentrations, which can be associated with high total Ca content, in MT100 samples may affect the Cr^{VI} release. Therefore, it is assumed that the mechanism controlling Cr^{VI}

release was sorption, according to the data from MT100 sample spiked with 1000 µg/L. Additional Cr^{VI} along with the naturally leached Cr^{VI} may the change balance between sorbate and sorbent, and the equilibrium for final Cr^{VI} concentration was reestablished at a different level.

The results Cr^{VI} measurements from sorption tests for 100% soil are listed in Table 11. During the other sorption tests, no sign of Cr^{VI} reduction was observed, hence analyzing solely hexavalent chromium concentration for soil was assumed to be adequate to examine the sorption capacity of soil. As seen in Figure 15, the affinity of soil for Cr^{VI} became zero at pH ~8. Sorbed portion of additional Cr^{VI} is estimated as 70 µg/L for soil at pH 6 and 125 µg/L Cr^{VI} at pH 4. It appears that soil had sorption capacity comparable to CP, which had presumably the highest sorption capacity, despite its relatively low oxalate-extractable Fe content of 890 mg/kg (corresponding 8.2% of its total Fe content) (Table 5). However, the background concentrations belonged to other oxyanions (e.g., As, P) that compete with Cr^{VI} for the same adsorption sites are much lower in the soil leachates. The results from oxalate extractions and WLTs demonstrated that soil had much lower total metal contents in solid phase and dissolved metal concentrations in its leachates (Table 6). For example, dissolved phosphate concentration from soil sample was below detection limit (MDL=50 mg/L) (Table 10) and there was 40 times more oxalate-extractable P in CP compared to soil (Table 9). Therefore, considering the significantly low background concentrations in leachates from 100% soil, FAs are likely much stronger sorbents compared to soil used in this study. Nevertheless, some of the mixtures contained up to 80% soil by mass and the limited sorption capacity of soil may have a minor influence on immobilization of oxyanions at trace levels.

The results of sorption tests showed that there were available capacity to sorb more Cr^{VI} than leached amount and thus Cr^{VI} should be immobilized almost completely under acidic conditions, especially in case of CP, which was an acidic fly ash (Mesuere and Fish 1992). This was confirmed by the detected Cr^{VI} concentrations below detection limit (MDL=10 µg/L) for BS and CP-containing samples at pH ~4.3. However, according to AAS analyses, BS100 and CP100 leached 13 and 19 µg/L TD Cr at pH ~4.3, suggesting that Cr leaching was primarily in form of Cr^{III} under acidic conditions. Trivalent chromium (Cr^{III}) is present as less soluble cation species, in contrast to highly soluble hexavalent chromium (Gao et al. 2005). Cr^{III} is likely associated with glassy matrix or aluminosilicate phases in fly ash (Goodarzi et al. 2008, Dudas and Warren 1987) and tend to form hydroxides in solution and readily precipitates, unless very strongly acidic conditions prevails (Fruchter et al. 1990, Gao et al. 2005).

In accordance with the discussion above, significant Cr^{III} leaching was not observed above pH 4.3. However, in numerous studies investigating mode of occurrence of Cr in fly ashes, including bituminous coal fly ashes from the Eastern U.S., it was reported that the predominant oxidation state of Cr is typically +III (>95%) (Huggins et al. 1999, Goodarzi et al. 2008, Shah et al. 2008, Nelson et al. 2010). According to the oxalate extraction data, 34-36% of total Cr content is associated to amorphous iron oxides for all fly ashes (Table 9). Considering higher solubility of Fe and other constituents of fly ash (e.g., silicate and Al) around pH 10 (Talbot et al. 1978, Gao et al. 2005), exhibited Cr leaching was relatively much lower and can be explained by predominant presence of Cr^{III}. The maximum observed Cr leachability values from BS100 and CP100 were 1.4% and 1.5% at pH ~10, respectively, whereas dissolved Cr concentration detected in MT100

leachate at pH 10.3 was 270 µg/L, which is corresponding to 8% Cr leachability for MT100 (Table 7). Cr leaching from BS100 and CP100 were 0.8 and 0.5% at pH ~4.3, respectively. It appears that possible oxidation of Cr^{III} induced Cr leaching. Especially, significantly higher Cr^{VI} leaching from MT-containing mixtures (Table 6), suggesting stronger oxidizing conditions or higher Cr^{VI} content in fly ash matrix compared to other samples. However, the available ORP (Oxidation Reduction Potential) data for WLTs without pH adjustment are around 120-150 mV (*p*e = 2−2.5) and very low to validate prevailing oxidizing conditions for Cr (Table 12) (Sparks 2003, Takeno 2005). But the measured ORP values may not be thermodynamically accurate (Komonweeraket 2010). On the other hand, significant Cr^{VI} leaching and complete recovery of spiked Cr^{VI} concentrations implies absence of reducing conditions.

Nevertheless, Cr leaching data as a function pH demonstrates that significant Cr release from sampled bituminous coal fly ashes and their mixtures with soil only occured in form of Cr^{VI}, which is the more toxic and mobile form of Cr (Soco and Kalembkiewicz 2009, Nelson et al. 2010). Alkaline conditions induced Cr^{VI} release, especially above pH 9, whereas it was retained on fly ash under acidic conditions.

3.4. Leaching Behavior of Arsenic

The As release from BS20 and BS30 was low (>12 µg/L) within the pH range of 4−6, whereas BS100 leached 54−56 µg As/L from pH 4 to 6.5 (Figure 16). When the pH value of these BS-containing samples was adjusted to ~7, dissolved As concentrations from BS20, BS30 and BS100 were all increased and become 9.5, 25 and 80 µg/L, respectively. Similarly, BSCP20 exhibited the lowest As leaching within the pH range of 4.30−5.88

(9.4−10 μg/L) and As concentration in the leachate increased to 23 μg/L at pH 7 (Figure 17). Furthermore, the same leaching pattern was also observed for CP (Figure 18) and MT-containing (Figure 19) mixtures. Arsenic release from CP30 and CP100 mixtures was low (3.1−13 μg/L for CP30; 2.5−11 μg/L for CP100) within the pH range of 4-7. Although available leaching data for MT-containing mixtures did not cover the pH range below 6, the lowest As concentrations measured for these samples were detected around pH 6.

Overall, the least amount of As from samples was leached within the pH range of 4−6 compared to alkaline pH ranges, suggesting that As release was predominantly in the form of As^{V}. Of the two stable oxidation state of As, As^{III} is highly soluble in natural aqueous systems and in fly ash leachates within the pH range of 4-10 due to its low sorption affinity (Turner 1981, Raven et al. 1998, Stollenwerk 2003). On the other hand, As^{V} has stronger sorption affinity for metal oxide surfaces, especially for amorphous iron oxides (van der Hoek and Comans 1996, Loeppert et al. 2002), similar to Cr^{VI}. Furthermore, in studies on coal fly ashes from various sources (Huggins et al. 2007, Shah et al. 2007) and bituminous fly ashes (Goodarzi and Huggins 2005, Goodarzi et al. 2008), the primary mode of occurrence of As in fly ash is reported as arsenate (>90%) with little presence of arsenite, and the predominant As species found in coal fly ash leachates was arsenate (Jackson and Miller 1998, Wang et al. 2009).

Arsenate is an oxyanion with 3 pKa points (Equation 10−12 (Stumm and Morgan 1996)), and it is predominantly present in form of $H_2AsO_4^-$ and $HAsO_4^{2-}$ within the pH range of 4-10. Arsenate adsorption onto amorphous iron surfaces can result surface complexes as

discussed earlier for Cr^{VI} (van der Hoek and Comans 1996, Yu 1997, Loeppert et al. 2002) (Equation 13)

$$H_3AsO_4 \xleftrightarrow{pK_{a1} = 2.26} HAsO_4^- + H^+ \quad (10)$$

$$HAsO_4^- \xleftrightarrow{pK_{a2} = 6.76} HAsO_4^{2-} + H^+ \quad (11)$$

$$HAsO_4^{2-} \xleftrightarrow{pK_{a3} = 11.29} AsO_4^{3-} + H^+ \quad (12)$$

$$\equiv FeOH^0 + H_2AsO_4^- + xH^+ \rightarrow \equiv FeOH_{x+1} \text{ --- } H_2AsO_4^{x-1} + H_2O \quad (13)$$

Although BS had a total As content of 24 mg/kg, which was less than half of the total As content of CP (52 mg/kg) (Table 2), BS100 leached higher amount of As, corresponding to As leachability of 4.5-6.6% compared to As leachability of 0.1-1.4% for CP100 within the pH range of 4-7. This significant difference between As retention capacity of two types of fly ashes can be attributed to the approximately 6 times higher amorphous iron oxide content of CP compared to BS (Table 9). Under acidic conditions, it is likely that the surfaces on CP100 particles still had available sorption sites for binding more As oxyanion, similar to its behavior observed during chromate sorption tests.

Within the pH range of 7−9, the As release from all mixtures were typically increased compared to the release within pH 4−7, except for MT100 (Table 6). The leached As concentrations from BS20 and 30 mixtures increased from 9.5 and 25 µg/L at pH 6.9 to 49 and 72 µg/L at pH 8.8, respectively. The As release from MT50 and MT60 increased from 25-27 µg/L at pH ~7.3 to 52 µg/L at pH ~9.3. Arsenıc leaching from CP100 sharply increased to 110 µg/L at pH 8.6. The similar leaching pattern was also observed for MT/Soil (Figure 19) and MT/FA/soil mixtures (Figure 17); arsenic release sharply

increased up to pH ~9. Moreover, from pH 7 to 9, the As release increased from all samples gradually, as the calculated percentage of $HAsO_4^{2-}$ relative to total dissolved As^V increased from 60% to 99%, but it appears that this considerable shift in distribution of species also contributed to the increase in As desorption, except for MT100 (Equation 8−10).

Above pH 9, the As leaching data are available only for CP30 and CP100; BS100; MT100 and MT/Soil mixtures. At this pH level, oxyanion affinity of metal oxides was assumed to be minimal, as observed during Cr^{VI} sorption tests, presumably due to oppositely charged As^V oxyanions and amorphous metal oxide surfaces. Therefore, As release as a result of desorption should reach its maximum level around pH 9−9.5. However, a sharp increase in As release was observed for BS100 and CP100 samples with further pH increase from ~9 to ~10. At pH 10−10.3, As releases from BS100 (Figure 16), CP100 and CP30 (Figure 18) were 373 µg/L (31% leachability), 408 µg/L (14% leachability) and 276 µg/L (30% leachability), respectively.

Significantly increased dissolved As concentrations from BS100, CP30 and CP100 may occur due to slightly elevated solubility of Fe in the glassy fly ash surface around pH 10 (Talbot et al. 1978, Dudas and Warren 1987, Gao et al. 2005). According to detected As concentrations from oxalate extracts, virtually all of the total As content of the three fly ashes were oxalate-extractable, suggesting As in fly ash was completely associated with amorphous Fe oxides (Table 9). Goodarzi and Huggins (2005) also determined that As was associated with the glass matrix in the surface of the particles rather than crystalline phases. Therefore, dissolution of Fe during weathering can release As and once released from fly ash matrix, As can form oxyanions that are highly mobile above pH 9. A similar

leaching pattern was not observed for Cr leaching from BS100 and CP100, possibly because of the predominant presence of Cr^{III} in fly ash (>95%). Cr^{III} should be oxidized first to become mobile under alkaline conditions (Gao et al. 2005). More importantly, approximately 2/3 of Cr was associated to less reactive phases, possibly aluminosilicate phases (Goodarzi et al. 2008) that was not oxalate-extractable according to Al concentrations from extracts below detection limit.

In contrast with increased As releases from CP100 and BS100, MT100 leached less As (63-70 µg/L) above pH 7, compared to its As release at pH 7 (90 µg/L) (Figure 19). Oxalate-exractable As concentrations implied similar As distribution and reactivity for all fly ashes (Table 9). Total As content of MT (52 mg/kg) was very close to total As content of CP (60 mg/kg) and approximately two times higher than total As content of BS (24 mg/kg) (Table 2). Despite of these findings, leachability of As from MT100 was relatively very low 2.7% at pH 10.3 (70 µg/L), compared to As leachability of CP100 and and BS100 at pH 10.3 (Table 7). Assuming sorption affinity of MT for oxyanions was negligible, the retention of As should be controlled by the solubility of a single or multiple types of solid phases.

The most significant difference, which can cause such a different arsenic leaching pattern, between MT and other FAs was its high total calcium (Table 2) and dissolved Ca contents (Table 4). The other studies investigated As leaching from fly ash reported that As release can be controlled by solubility of a Ca-As phase at alkaline conditions, in the presence of high Ca levels (van der Hoek et al. 1994, Quero et al. 2001, Wang et al. 2009). As and Ca can form many different low-solubility compounds, such as $Ca_4(OH)_2(AsO_4)_2 \cdot 4H_2O$, $Ca_5(AsO_4)_3 \cdot OH$ (arsenate apatite), $Ca_3(AsO_4)_2 \cdot 6H_2O$,

$Ca_3(AsO_4)_2 \cdot 10H_2O$, and $CaNaAsO_4 \cdot 7.5H_2O$ (Bothe and Brown 1999, Wang, et al. 2009). Furthermore, inorganic phosphate species have a configuration that is identical to As^V (Wagemann 1978, Loeppert et al. 2002) and a similar solubility control was observed for phosphate in MT mixtures (Table 10). In Figure 14, the P leaching from MT100 and MT/Soil samples decreased approximately 25% within the pH range of 9.3−9.8. At pH 9.83, As and P releases from MT100 were 52 µg/L and 89 µg/L, respectively, and dissolved Ca concentration in this leachate was 90 mg/L (Table 4). It is hard to calculate the saturation level for the solid As phases, since the fly ash systems are rather complex, but these values may give an insight for the saturation limits of solid Ca-As and Ca-P phases..

Other MT-containing mixtures (MT/Soil and MT/FA/Soil) did not exhibit decreased As release under alkaline conditions. Dissolved As concentrations from these samples increased gradually with increasing pH, suggesting that their leachates were not saturated to As-Ca phases. It appears that Ca concentrations below 58 mg/L did not cause saturation of As-Ca phases (Table 4), but P leaching from these samples also decreased within the pH range of 9.3−9.8 (Figure 13).

3.5. Leaching Behavior of Copper

Dissolved Cu concentrations detected from BS100 and BS/Soil samples with soil are plotted in Figure 20 as function of leachate pH. Among all samples, the highest dissolved Cu concentration, 490 µg/L (17% leachability), was measured from BS100 at pH 4.3 (Table 6). Other BS/soil mixtures, BS20 and BS30, leached 89 and 160 µg/L of Cu, respectively, around pH 4.3. Fruchter et al. (1990) determined that CuO (tenorite), which

is a likely mode of occurrence of Cu in fly ashes, is the solubility-controlling phase. The dissolution of CuO, which is favored under acidic conditions (Equation 14), explains the high Cu release at pH ~4.3.

$$CuO_{(s)} + H^{+} \leftrightarrow Cu^{2+} + OH^{-} \quad (14)$$

The oxalate-extractable Cu content of all fly ashes corresponded to around 35% of their total Cu content (Table 9), suggesting a similar distribution and leachability of Cu under acidic conditions (pH=3) for all fly ashes. Accordantly, the maximum Cu leaching from BS100 and CP100 was observed under acidic conditions (Table 7). he dissolved Cu concentration from CP100 at its natural pH of 4.41 was 67 µg/L (1.9% leachability) (Figure 21). However, after the leachate pH of CP100 was brought to 4.27 via HNO_3 addition, Cu concentration decreased to 3.1 µg/L in contrast to the high release that was observed in case of BS-containing mixtures (Figure 20). The same pattern was also observed for BSCP20 (Figure 22). Cu leaching from BSCP20 was 4.4 µg/L at pH 5.88 and at pH 4.30 it leached 7.2 µg/L, which was significantly lower than the Cu release from BS20 at pH ~4.3. The difference in leaching behavior might be caused by the high unburned carbon content (LOI) of CP compared to BS (4.4% vis-à-vis 10.5% (Table 1)). Unburned carbon in fly ash matrix has a porous structure which provides large surface area and can bind Cu even under acidic conditions (Lin and Chang 2001). However, this behavior was not exhibited by CP30. When its natural pH (pH 5.32) was decreased to ~4.3, the dissolved Cu concentration from CP30 was 190 µg/L, which was even higher than leaching from BS30. Therefore, the possible effect of unburned carbon content on Cu leaching can not be specified through the available data.

Above pH ~4.3, Cu leaching from pure BS and CP and their mixtures with soil become significantly lower (≥24 µg/L), showing little fluctuation with increasing pH. Similarly, MT/FA/Soil (Figure 22) and MT/Soil mixtures (Figure 23) leached only equal to or below 14 µg Cu/L within the pH range of ~6 to ~10. Despite of the fluctuation in leached Cu concentrations (15−55 µg/L), Cu leaching from MT100 also decreased and became insignificant (≤2.1 µg/L) similar to BS100 and CP100 around pH 10 (Figure 23).

Under acidic conditions, Cu^{2+} becomes the predominant form of Cu in solution, hence Cu mobility is high (Reddy et al. 1995). As pH increases from acidic to neutral range, positively charged Cu species can be sorbed onto metal oxide surfaces and sorption efficiency reaches 100% around pH 6−7 (Benjamin 1983, Coughlin and Stone 1995, Hèquet et al. 2001, Zhu 2002,). Sorption of Cu onto metal oxide surfaces may be explained by the opposing charges on the ions and the binding site, similar to the pH-dependent sorption of As and Cr^{VI} (Equations 15−16). According to the sorption capacity analyses on Cr^{VI}, sorption affinity for cations should be very high at alkaline conditions. With further pH increase towards neutral range, Cu activity decreased due to the formation of less soluble Cu hydroxides ($Cu(OH)_2$) (Evans 1989, Benjamin 1983), as shown in Equation 17. Additionally, Cu can form complexes with a large variety of ligands (e.g., $CuCO_3$, $CuSO_4$) and precipitate (Turner et al. 1981, Al-Abed et al. 2006, Komonweeraket 2010). Around neutral pH range, the sorption affinity of Cu onto metal oxides and unburned carbon become less prominent and the removal of Cu from solution may be dominated by precipitation of Cu hydroxides (Hèquet et al. 2001, Lin and Chang 2001). Lastly, the solubility of CuO decreases significantly at high pH values (Fruchter et al. 1990) (Equation 14). Therefore, it is possible that Cu in the fly ash was not released

significantly at all and this can explain further decreased Cu leaching around pH 10, in addition to Cu hydroxide precipitation and strong sorption affinity of metal oxides for cations at high pH.

Overall, even if it is initially released from fly ash surface due to weathering, the Cu in the solution could be removed from the solution through the mechanisms discussed above at equilibrium.

$$\equiv Me{-}OH^{0} + Cu^{2+} \leftrightarrow \equiv Me{-}O^{-}\text{---}Cu^{2+} + H^{+} \quad (15)$$

$$\equiv Me{-}OH^{0} + CuOH^{+} \leftrightarrow \equiv Me{-}O^{-}\text{---}CuOH^{+} + H^{+} \quad (16)$$

$$Cu^{2+} + 2\ OH^{-} \leftrightarrow Cu(OH)_{2\ (s)} \quad (17)$$

The fluctuation in Cu concentrations from MT100 was possibly due to its high soluble Ca content and high levels of buffer solution addition. The higher level of total dissolved solids in MT100 leachates were reflected in 20-60% higher EC values (3.61-5.93 mS/cm) on the average compared to EC values for BS and CP-containing mixtures. As discussed earlier, MT had higher acid neutralizing capacity and because of that, higher buffer concentrations were required to adjust pH to the desired values. During WLTs, the highest amount of buffer (0.05 M) was added to MT100 samples for fixing their final pH to 7.29 and 9.40. 0.05 M buffer addition corresponds to 0.006-0.022 M Na^{+} in addition to 0.02 M Na^{+} in the blank solution. As seen in Figure 23, the highest dissolved Cu concentrations from MT100 were also detected in leachates with pH 7.29 (55 µg/L) and pH 9.40 (49 µg/L), implying a possible correlation between induced Cu leaching and higher dissolved cation concentrations (e.g., Na^{+} and Ca^{2+}). Cations can compete for the same sorption site (Stumm and Morgan 1996). Therefore, significantly higher Na^{+} and

Ca^{2+} concentrations in MT100 samples compared to all other samples may interfere with precipitation and sorption of Cu species and caused more Cu release for some of the MT100 samples with pH adjustments.

4. SUMMARY AND CONCLUSIONS

The fly ashes obtained from three coal-fired power plants in Maryland were utilized at highest possible amounts to prepare soil/fly ash mixtures that meet the regulated compaction limit of 100 lb/ft^3 by the Maryland State Highway Administration. The leaching potentials of the pure FAs and their mixtures with soil were analyzed for copper, arsenic, and chromium within the pH range of 4−10. Despite the complexity of the solid-liquid partitioning, the dominant mechanisms controlling trace metal leaching at different pH ranges were determined for most of the samples. The following conclusions were made based on general leaching trends for the samples:

- A strong correlation is noted between leachate pH and the ratio of dissolved calcium concentration (a surrogate for dissolved CaO) to oxalate-extractable Fe concentration (a surrogate for amorphous iron oxides) (R^2=0.84). This correlation demonstrates that the pH of the leachate is subject to significant change over time due to weathering of amorphous iron oxides and CaO.
- Copper (Cu) leached significantly only under acidic conditions (pH ~4.3). Beyond pH ~4.3, dissolved Cu concentrations were likely to be decreased through precipitation as hydroxides and sorption onto metal oxides or unburned carbon. However, the type of mechanism predominantly governed Cu leaching cannot be specified.
- The predominant oxidation state of chromium (Cr) in the leachates was determined as Cr^{VI}, with the exception of Cr^{III} release at pH ~4.3. Accordantly to its oxyanion form, Cr was efficiently immobilized below pH 7 presumably by amorphous iron oxide surfaces and dissolved Cr concentrations increased monotonically as pH further increased above 7 without any indication of saturation.

- The observed leaching behavior of arsenic could be best explained by leaching predominantly in the form of As^{V}. Arsenic release typically followed a trend similar to Cr release; strong retention pH<7 and increased leaching with increasing pH. Arsenic was strongly associated with amorphous Fe oxide content and significantly higher As release around pH 10 compared to leaching at pH 7−9 implies that slightly higher solubility iron oxides under strong alkaline conditions may also contribute to As release, along with desorption of As. Decreased As concentrations above pH 9 was only observed for MT100, which had the highest dissolved Ca concentration (90 mg/L), implies possible solubility control by Ca-As phases.
- The most successful mixture was BSCP20, which had a natural leachate pH ~6, in terms of environmental safety (i.e., low leaching risk) and compactability, while replacing maximum amount of natural aggregate (i.e., soil). BSCP20 was composed of 20% BS, 20% CP (40% FA in total) and 60% soil by mass and still met the 100 lb/ft^3 dry unit weight limit. MT could be used up to 60% by mass in FA/soil mixtures while meeting the regulated limit, but the leachates from MT-containing mixtures had natural pH values above 9, where mobility of toxic Cr^{VI} species are high.

APPENDIX A: TABLES

Table 1. Physical and chemical properties of soil and fly ashes.

Material	Specific Gravity	Optimum Water Content (%)	Maximum Dry Unit Weight (lb/ft^3)	LOI [1] (%)	Leachate pH [2]	Moisture Content (%)	ASTM C618 Class
Soil	2.6	11	122	0.9	5.32	0.24	- -
Brandon Shores	2.3	16	76	4.4	6.53	0.17	Class F
Morgantown	2.4	25	84	7.3	9.83	0.40	Off-Spec
Chalk Point	2.2	no data	no data	10.5	4.41	0.28	Off-Spec

[1]: LOI: Loss on ignition

[2]: Geometric average of pH measurements from triplicate WLTs.

Table 2. Total elemental analysis (TEA) results conducted on soils and fly ashes by University of Wisconsin Soil Testing and Plant Analysis Laboratories. All concentrations are reported as mg/kg dry weight.

Element	Soil	Brandon Shores	Morgantown	Chalk Point
Ag	< 0.001	0.001	< 0.001	< 0.001
Al	28800	21300	29100	26300
As	< 3	24	52	60
B	2.9	21	240	27
Ca	280	2200	10100	3300
Cd	<0.4	0.4	1.6	0.7
Co	4.6	21	10	17
Cr	16	50	68	49
Cu	1.3	60	36	54
Fe	10800	6400	24600	26500
Hg	< 0.001	< 0.001	< 0.001	< 0.001
K	550	3700	4500	6500
Li	4	36	31	30
Mg	370	1000	5800	1500
Mn	38	34	210	280
Mo	< 0.4	12	17	9.4
Na	33	540	2400	720
Ni	< 0.3	21	< 0.3	< 0.3
P	160	370	640	370
Pb	< 2	23	8.8	11
S	69	820	3900	2200
Sb	0.022	0.048	0.009	0.005
Tl	< 0.001	< 0.001	< 0.001	< 0.001
V	17	79	140	66
Zn	15	54	84	32

Table 3. Standard Proctor Test (ASTM D698) results for FA/soil mixtures at different proportions.

Mixture [1]	Fly Ash Content [2] (%)			Soil Content [3] (%)	Optimum Water Content (%)	Maximum Dry Unit Weight (lb/ft^3)
	BS	CP	MT			
SOIL	--	--	--	100	11	122
Brandon Shores + Soil Mixtures						
BS 20	20	--	--	80	11	120
BS 30	30	--	--	70	11	112
BS 100	100	--	--	--	16	76
Chalk Point + Soil Mixtures						
CP 30	--	30	--	70	13	110
CP 100	--	100	--	--	no data	no data
Morgantown + Soil Mixtures						
MT 50	--	--	50	50	13	111
MT 60	--	--	60	40	15	104
MT 100	--	--	100	--	25	84
2 FAs + Soil Mixtures						
BS 20 - CP 20	20	20	--	60	14	105
CP 25 - MT 25	--	25	25	50	15	102
MT 25 - BS 25	25	--	25	50	13	106

[1] : BS: Brandon Shores fly ash, CP: Chalk Point, MT: Morgantown, SOIL: Soil w/o fly ash. The numbers after the abbreviation designate the percentage of fly ash by weight in the mixture. Some mixtures consist of two different types of fly ashes at equal amounts (by weight).

[2] : Percentage of fly ash content by weight in the mixture.

[3] : Percentage of soil content by weight in the mixture.

Table 4. Oxalate-extractable Fe and dissolved Ca contents per dry unit weight for WLTs without pH adjustment.

Mixture	pH [1]	EC (mS/cm @25C)	Dissolved Calcium Concentration (mg/L)	Dissolved Ca Content (mg/kg) [2]	Oxalate-Extractable Fe Content (mg/kg) [3]	Dissolved Ca: Oxalate-Extractable Fe [4]
BS 20	5.57	2.58	6.8 ±0.3	0.14	1100	1.3 E-04
BS 30	5.76	2.70	7.4 ±0.2	0.15	1100	1.3 E-04
BS 100	6.53	2.78	12 ±0.4	0.25	1700	1.5 E-04
MT 50	9.57	3.12	50 ±1.4	1.01	3100	3.3 E-04
MT 60	9.73	3.22	58 ±0.5	1.15	3600	3.2 E-04
MT 100	9.83	3.66	90 ±2.2	1.80	5300	3.4 E-04
MTBS25	9.26	2.90	28 ±0.3	0.55	2200	2.5 E-04
CPMT25	8.94	3.00	30 ±0.3	0.61	4400	1.4 E-04
BSCP20	5.90	2.71	12 ±0.2	0.23	3000	7.7 E-05
CP 30	5.32	2.97	13 ±0.6	0.26	3800	6.8 E-05
CP 100	4.41	2.96	30 ±0.7	0.60	10600	5.7 E-05
SOIL	5.32	2.56	4.7±0.2	0.09	890	1.0 E-04
BS 40 *	6.21	2.70	8.2±0.3	0.16	1200	1.3 E-04
CP 40 *	4.34	2.83	16 ±1.4	0.32	4800	6.7 E-05
MT 40 *	9.50	3.12	46 ±0.7	0.92	2700	3.5 E-04

[1] : Geometric mean of pH values from triplicate WLT leachates.

[2] : Calculated by using the average of measured dissolved Ca concentrations.

[3] : Estimated using dilution calculations by using the pure material's Fe concentration in oxalate extracts.

[4] : Dissolved Ca content (mg/kg) over oxalate-extractable Fe content (mg/kg).

* **:** Mixtures that were only testes for dissolved Ca.

Table 5. Dissolved Fe concentrations from ammonium oxalate extracts (pH=3, S:L= 1:40 g/mL).

Material[1]	Dissolved Fe Concentration in Oxalate Extracts (mg/L) [2]	Oxalate-Extractable Fe [3] (mg/kg)	Total Fe Content (mg/kg) [3, 4]	Oxalate Extractable-to-Total Content Ratio (%) [5]
Soil	22 ±6.3	890	10800	8.2
BS	42 ±8.8	1700	6400	27
CP	270 ± 22	10600	26500	40
MT	130 ± 26	5300	24600	21

[1] : BS: Brandon Shores fly ash, CP: Chalk Point fly ash, MT: Morgantown fly ash, SOIL: Soil w/o fly ash.

[2] : Average dissolved Fe concentrations from triplicate ammonium oxalate extractions with standard deviations

[3] : mg trace metal per kg soil based on dry unit weight

[4] : Total Fe content from TEA (Table 2).

[5] : Percentage of Oxalate-extractable Fe content relative to total Fe content.

Table 6. Results of triplicate Water Leach Tests (WLT) on the prepared mixtures. Concentrations of dissolved Cu, total Cr, Cr^{VI} and As in the leachates are given with standard deviation.

Mixture	pH	EC (mS/cm @25C)	Dissolved Metal Concentrations in the Leachates (µg/L) [1]				Cr^{VI}: TOT Cr (%) [4]
			Copper	Arsenic	TD Cr [2]	Cr^{VI} [3]	
BS20	4.32	2.45	89 ±5.8	5.6 ±0.0	3 ±0.2	<10	- -
	5.57*	2.59	1.6 ±0.6	0.7 ±0.2	1 ±0.2	no data	- -
	6.93	2.79	2.6 ±0.2	25 ±2.6	3.4 ±0.2	no data	- -
	8.77	2.59	1.4 ±0.5	49 ±4.9	4.2 ±0.5	<10	- -
BS30	4.22	2.49	160 ±7.9	12 ±0.1	6.7 ±0.2	<10	- -
	5.76*	2.70	1.2 ±0.1	1.2 ±0.1	1.5 ±0.2	no data	- -
	6.93	2.79	1.6 ±0.3	9.5 ±0.7	2.2 ±0.2	no data	- -
	8.83	2.62	1.9 ±0.0	77 ±2.4	6.4 ±2.5	<10	- -
BS100	4.29	2.66	490 ± 11	56 ±0.6	19 ±2.3	<10	- -
	6.53*	2.78	0.7 ±0.2	54 ±5.4	6.8 ±0.5	<10	- -
	7.03	3.01	24 ±0.5	80 ±1.2	7.5 ±0.2	<10	- -
	8.18	3.04	2.1 ±0.2	110 ±2.1	16 ±0.3	<10	- -
	8.77	2.78	5.2 ±0.5	110 ±5.1	22 ±0.5	21 ±1.1	95
	10.27	2.91	2.1 ±0.7	370 ±4.2	37 ±0.7	39 ±2.8	105
MT50	6.23	3.53	3.8 ±1.0	7.9 ±0.5	79 ±4.1	110 ±2.4	139
	7.31	4.34	10 ±2.2	25 ±0.7	78 ±3.6	90 ±2.8	115
	9.35	3.16	12 ±2.4	52 ±5.0	120 ±15	130 ±2.4	108
	9.57*	3.12	<0.4	62 ±18	120 ±12	130 ±7.4	108
MT60	6.19	3.42	6.9 ±4.7	8.4±0.6	97 ±6.3	130 ±4.6	134
	7.34	3.95	11 ±2.3	27 ±1.9	110 ±23	98 ±18	89
	9.35	3.52	11 ±3.3	52 ±8.6	140 ±22	160 ±2.5	114
	9.73*	3.22	<0.4	81 ±11	150 ±14	160 ±7.4	107
MT100	6.17	4.58	15 ±2.7	26 ±1.0	110 ±3.0	130 ±3.2	118
	7.29	5.63	55 ±3.0	90 ±8.3	97 ±2.2	85 ±1.8	88
	7.44	4.94	29 ±1.7	63 ±2.5	160 ±1.1	180 ±4.7	113
	7.91	4.54	17 ±0.6	no data	170 ±0.1	180 ±0.0	106
	9.40	3.61	49 ±0.6	65 ±17	240 ±0.9	210 ±2.5	88
	9.83*	3.66	<0.4	52 ±12	230 ±11	250 ±8.0	109
	10.32	3.91	1.6 ±0.1	70±4.2	270 ±5.0	230 ±10	85

Table 6. Results of triplicate Water Leach Tests (WLT) on the prepared mixtures (*continued*).

Mixture	pH	EC (mS/cm @25C)	Dissolved Metal Concentrations in the Leachates (µg/L) [1]				Cr^{VI}: TD Cr (%) [4]
			Copper	Arsenic	TD Cr [2]	Cr^{VI} [3]	
MTBS25	5.90	3.31	6.3±2.6	13 ±0.1	40 ±2.1	46 ±1.9	115
	7.22	3.67	14 ±3.4	22 ±1.5	42 ±3.8	51 ±1.0	121
	9.09	2.91	6.3±0.4	no data	52 ±3.5	70 ±3.8	135
	9.25*	2.89	<0.4	69 ±11	67 ±9.4	79 ±0.6	118
CPMT25	5.90	3.30	2.7±0.2	9 ±0.2	28 ±0.4	28 ±4.2	100
	7.28	3.59	8.6±1.0	22 ±5.5	49 ±5.9	49 ±2.6	100
	8.94*	3.00	<0.4	73 ±17	73 ±9.0	75 ±9.3	103
	9.00	3.04	3.2±0.4	96 ±7.8	63 ±5.0	69 ±1.9	110
BSCP20	4.30	2.51	7.2±3.1	9.4±1.2	4.4±0.3	<10	- -
	5.88*	2.70	4.4±0.4	10 ±5.5	1.0±0.2	no data	- -
	7.00	2.96	4.2±0.8	23 ±3.1	3.1±0.2	<10	- -
	8.74	2.70	<0.4	no data	7.6±0.3	<10	- -
CP30	4.25	2.57	190 ±22	11 ±0.9	5.7±0.7	<10	- -
	5.32*	2.97	2.5±0.7	3.1±1.6	<0.6	no data	- -
	6.92	2.95	1.3±0.4	13 ±1.4	4.3±0.5	no data	- -
	10.02	2.74	1.1±0.3	280 ±8.4	13 ±1.3	<10	- -
CP100	4.27	2.84	3.1±0.6	11 ±1.5	13 ±0.3	<10	- -
	4.41*	2.96	67 ±11	2.5±0.9	4 ±101	no data	- -
	6.96	3.61	5.3±0.7	6.2±0.8	5 ±0.1	<10	- -
	8.62	3.12	24 ±18	110 ±29	23 ±31	18 ±0.8	78
	10.10	3.23	1.7±0.1	410 ±2.7	33 ±1.1	16 ±6.1	48
SOIL	4.36	2.36	80 ±2.3	2.6 ±0.2	<0.6	no data	- -
	5.32*	2.56	<0.4	<0.4	<0.6	<10	- -
	7.00	2.70	<0.4	<0.4	<0.6	no data	- -
	10.08	2.54	<0.4	3.3±0.2	<0.6	no data	- -

[1] : Method detection limit (MDL) for Cu, Cr and As were 0.4 µg/L, 0.4 µg/L and 0.6 µg/L, respectively.

[2] : Average total dissolved chromium concentration from AAS analyses.

[3] : Average dissolved hexavalent chromium concentration from UV-Vis spectrophotometry analyses. Method detection limit for Cr^{VI} =10 µg/L.

[4] : The percentage of hexavalent chromium concentration relative to total dissolved chromium concentration.

* **:** Natural pH of the leachate from WLT runs without pH adjustment.

Table 7. Maximum leachability of trace metals from Water Leach Tests (WLTs).

Mixture	Maximum Cu Leachability (%)	Maximum Cr Leachability (%)	Maximum As Leachability (%)
BS100	17 (pH 4.3)	1.5 (pH 10.3)	31 (pH 10.3)
MT100	3.1 (pH 7.3)	8.0 (pH 10.3)	3.4 (pH 7.3)
CP100	2.5 (pH 4.4)	1.4 (pH 10.1)	14 (pH 10.1)
SOIL	125 (pH 4.3)	0.03 (pH 10.0)	4.4 (pH 10.0)

Note: Leachability of trace metals calculated using Equations 5 and 6. pH values within parentheses are designated for the geometric mean of the leachate pH.

Table 8. Residual chromium concentrations from triplicate sorption tests conducted as WLTs spiked with Cr^{VI}.

Label	pH	EC [1] (mS/cm)	Residual Chromium Concentration (µg/L)		Cr^{VI}: TD Cr (%) [4]
			TD Cr [2]	Cr^{VI} [3]	
Blank [5]	5.49	2.54	250 ±0.9	250 ±4.6	100
BS100 [5]	5.60	3.07	180 ±1.6	190 ±1.1	95
	6.77	2.85	190 ±3.3	200 ±4.1	95
	7.05	2.82	160 ±6.3	200 ±6.2	80
	8.16	2.99	260 ±8.5	260 ± 12	100
	8.67	2.84	320 ± 37	300 ± 48	107
	10.31	2.73	310 ±6.5	300 ±1.6	103
CP100 [5]	4.29	3.01	8 ±0.5	<10	- -
	5.51	3.29	68 ±2.9	68 ±2.1	100
	6.90	3.40	97 ±0.5	120 ±2.3	81
	8.31	2.93	240 ±6.6	210 ±4.2	114
	9.78	3.20	280 ±7.4	260 ±0.3	108
MT100 [5]	6.09	4.72	320 ±2.4	320 ±5.3	100
	7.42	5.24	290 ±7.1	430 ±9.0	67
	7.99	3.90	340 ±8.6	330 ±4.3	97
	9.14	3.74	240 ±3.4	390 ±3.6	62
	9.79	3.73	360 ±3.3	360 ± 12	100
MT100-1000 [6]	9.14	3.57	860 ±150	860 ±140	100

[1]: Electrical conductivity of filtered leachate compensated for 25°C.

[2]: Average total dissolved chromium concentration from AAS analyses. Method detection limit for Cr = 0.6 µg/L.

[3]: Average dissolved hexavalent chromium concentration from UV-Vis spectrophotometry analyses. Method detection limit for Cr^{VI} = 10 µg/L.

[4]: The calculated ratio of hexavalent chromium concentration (µg/L) over total dissolved chromium (µg/L).

[5]: Triplicate samples spiked with 250 µg Cr^{VI}/L.

[6]: Triplicate MT100 sample spiked with 1000 µg Cr^{VI}/L.

Table 9. The oxalate-extracted As, Cu Cr and P concentrations for pure soil and fly ash samples (BS, CP and MT). Triplicate ammonium oxalate extractions were conducted using solid-to-liquid ratio of 1:40 g/mL at pH=3.

Element	Material	Dissolved Metal Concentration in Oxalate Extracts (µg/L) [1]	Oxalate Extractable Content (mg/kg) [2]	Total Metal Content (mg/kg) [3]	Oxalate Extractable-to-Total Content Ratio (%) [4]
Cu	Soil	24 ±8.4	1.0	1.3	74
	BS	760 ± 33	30	60	50
	CP	570 ± 15	23	54	43
	MT	410 ± 37	16	36	44
Cr	Soil	29 ± 6.7	1.2	16	7.3
	BS	420 ± 14	17	50	34
	CP	420 ± 4.5	17	49	35
	MT	610 ± 21	24	68	35
As	Soil	27 ±8.0	1.1	1.5 *	72
	BS	750 ± 26	30	24	125
	CP	1600 ± 13	64	60	107
	MT	1300 ± 43	52	52	100
P	Soil	53 ± 9	2.1	160	1.3
	BS	1500 ±140	59	370	16
	CP	2100 ± 82	84	370	23
	MT	2500 ±250	100	640	16

[1]: Average element concentrations from triplicate filtered ammonium oxalate extracts with the standard deviations.

[2]: Calculated oxalate-extractable content per unit weight of the solid material.

[3]: Total elemental content from total elemental analysis (TEA) (Table 2)

[4]: The percentage of oxalate-extractable content (mg/kg) relative to total content (mg/kg).

*: ½ of reported detection limit for total As content from TEA.

Table 10. Dissolved phosphate concentration in same of the WLTs (S:L=1:20) (MDL = 50 µg/L).

Mixture	pH	Dissolved P Concentration (µg/L)
BS100	6.53	160 ± 19
BSCP20	5.88	76 ± 2.8
CP100	4.41	63 ± 7.5
CP100	6.96	96 ± 14
CPMT25	8.94	94 ± 0
MT100	9.83	89 ± 7
MT100	7.29	230 ± 87
MT100	9.40	110 ± 0
MT100	6.17	120 ± 26
MT50	9.57	95 ± 12
MT50	7.31	96 ± 14
MT50	9.35	110 ± 20
MT60	9.73	94 ± 9.9
MT60	9.35	130 ± 24
MTBS25	9.25	120 ± 12
SAND	7.01	<50

Table 11. Residual hexavalent chromium concentrations from sorption tests conducted as WLTs spiked with Cr^{VI} for 100% Soil samples.

Label	*n* [1]	pH	EC (m*S*/cm)	Residual Hexavalent Chromium Concentration (µg/L)
Blank [2]	3	5.58	2.6	250 ±3.1
SOIL [2]	3	4.83	2.52	110 ±1.7
	3	5.05	2.54	120 ±2.1
	1	5.13	6.13	120
	3	5.55	2.66	140 ±2.4
	3	5.64	2.53	130 ±1.7
	1	5.68	2.6	130
	3	6.08	2.71	170 ±0.7
	3	6.88	2.6	200 ±4.9
	1	6.98	2.55	210
	1	7.98	2.57	250
	1	8.42	2.56	250
	1	8.61	2.6	250
	3	8.76	2.6	250 ±1.5

[1]: Number of replicates

[2]: Samples spiked with 250 µg Cr^{VI}/L

Table 12. Oxidation reduction potential (ORP) measurements from WLTs without pH adjustment.

Mixture	E_h (mV)
BS20	147 ± 1.8
BS30	132 ± 2.3
BS100	no data
MT50	126 ± 6.4
MT60	119 ± 8.2
MT100	122 ± 4.3
MTBS25	142 ± 13
CPMT25	146 ± 9.4
BSCP20	145 ± 5.7
CP30	121 ± 0.5
CP100	152 ± 7.0

APPENDIX B: FIGURES

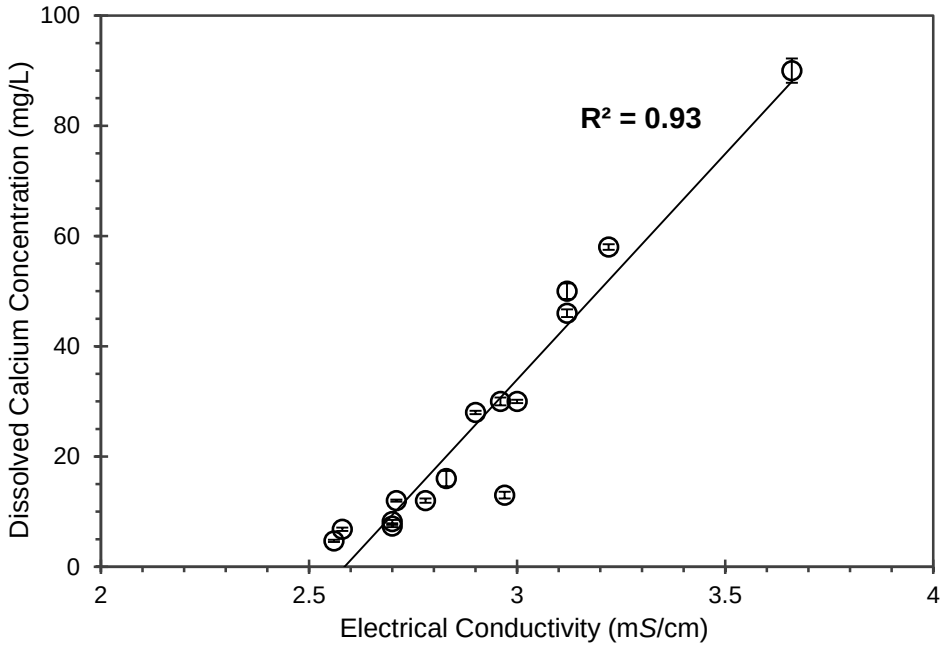

Figure 1. Electrical conductivity (millisiemens/cm @ 25°C) of the filtered leachates versus dissolved Ca concentration from WLT samples without pH adjustment (S:L = 1:20 g/mL, MDL=0.05 mg/L).

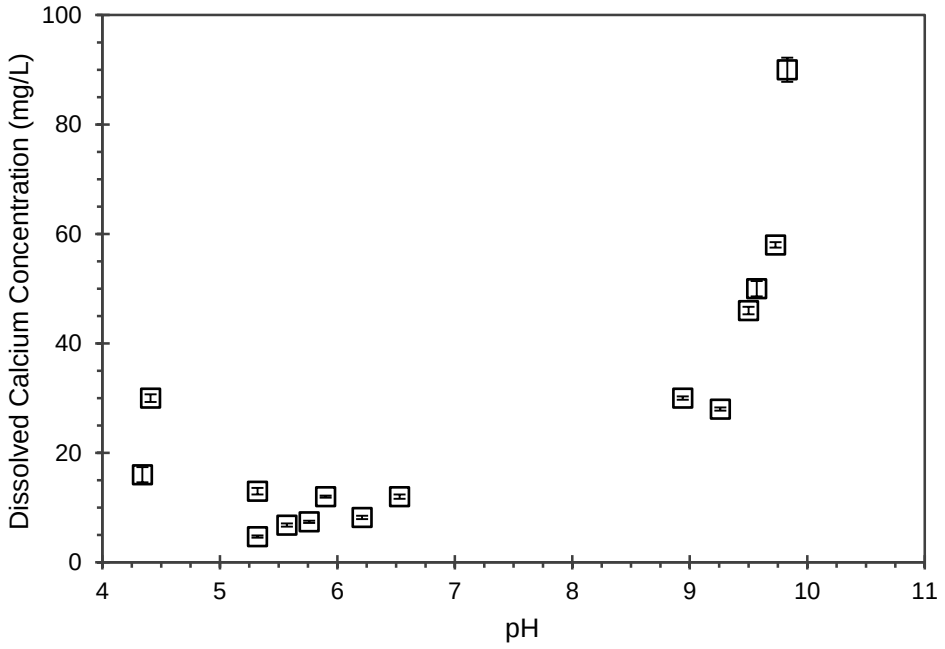

Figure 2. The pH of the leachate versus dissolved Ca concentration from WLT samples without pH adjustment (S:L = 1:20 g/mL, MDL=0.05 mg/L).

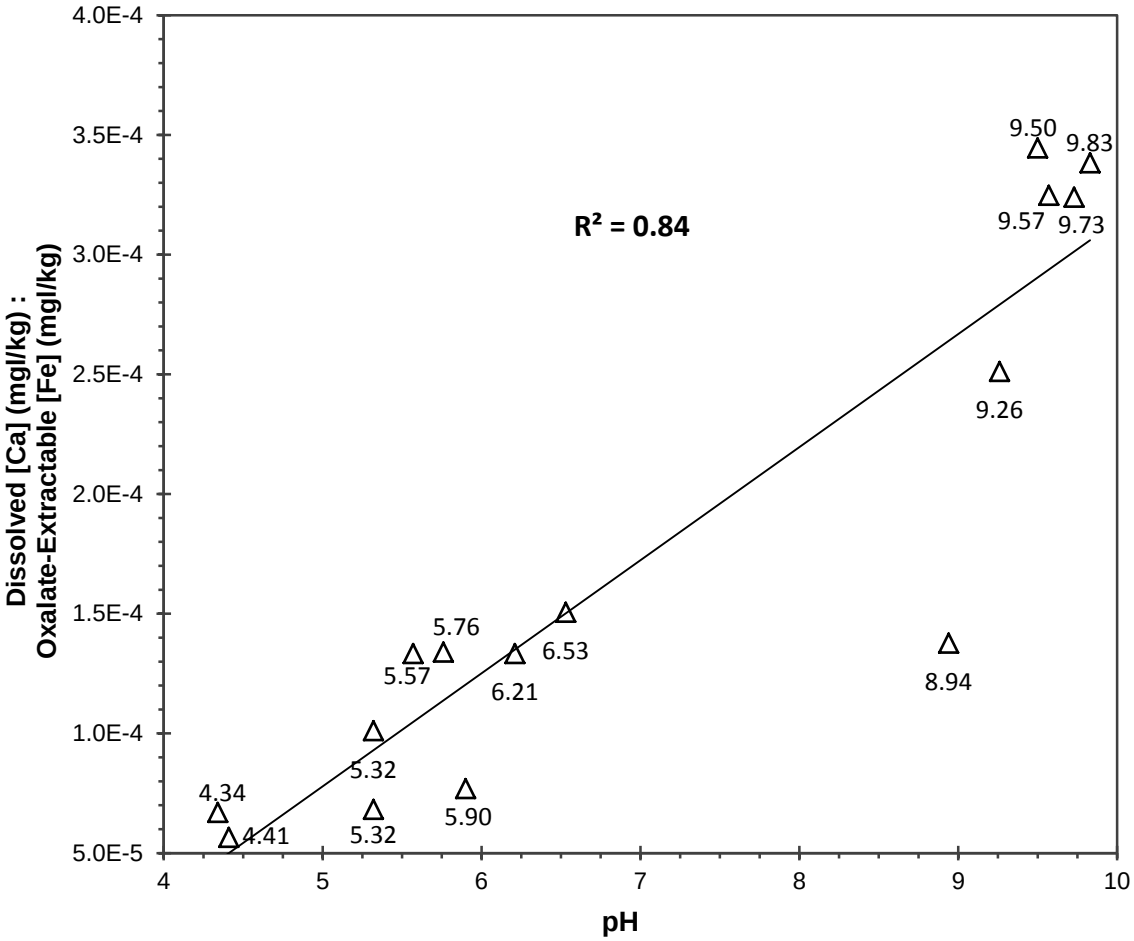

Figure 3. Soluble Ca content (mg/kg) over oxalate-extractable Fe concent (mg/kg) of the samples versus leachate pH value of the samples (given as labels near data points). Oxalate-extractable Fe content was estimated using Equation 1. Dissolved Ca content was calculated using dissolved Ca concentrations from WLTs without pH adjustment (S:L=1:20 g/mL).

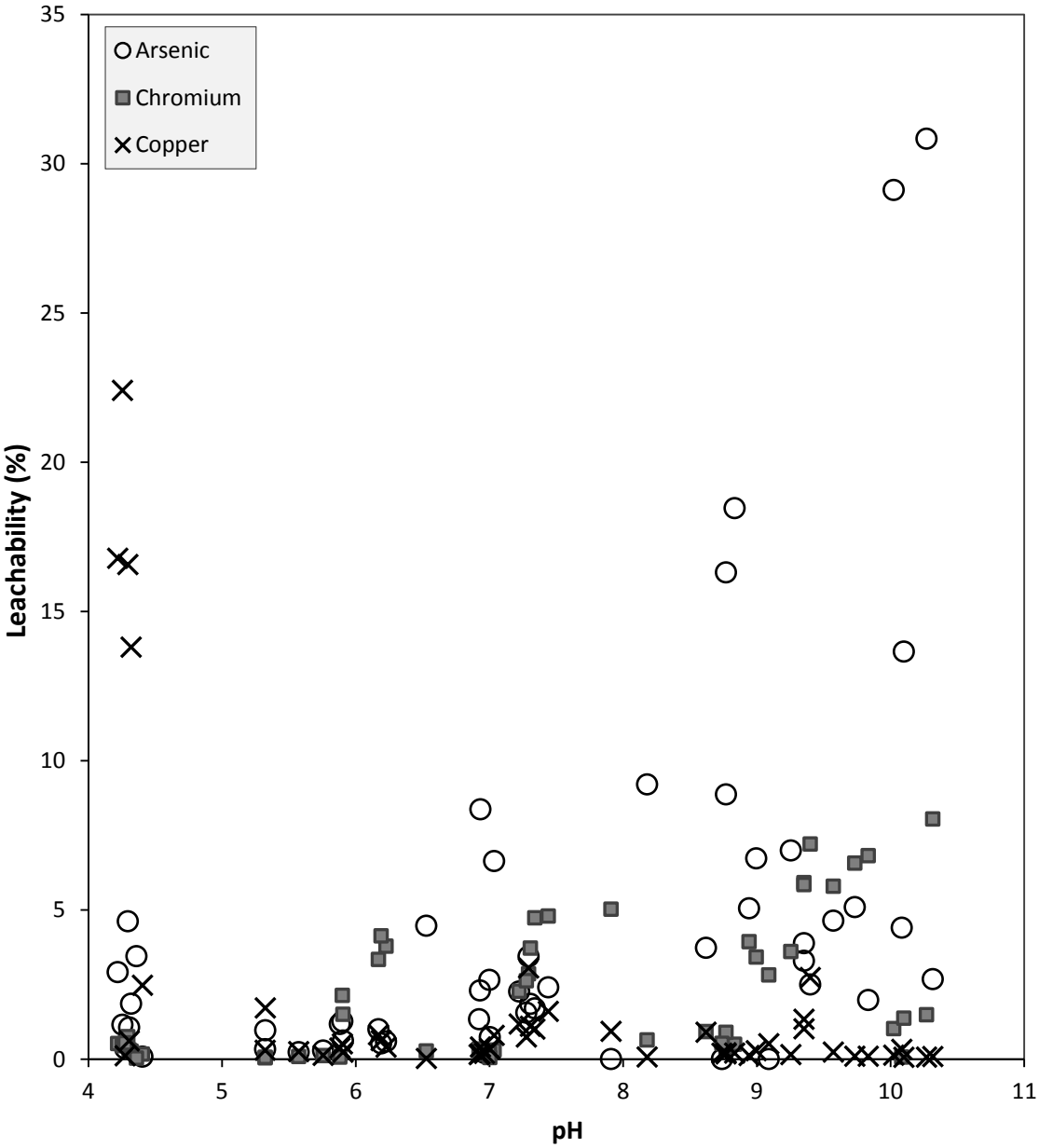

Figure 4. The leachability of arsenic, copper and chromium for all of the samples. Leachability is calculated using Equations 5 and 6. High Cu leachability (125%) for 100% soil at pH ~4.3 is excluded.

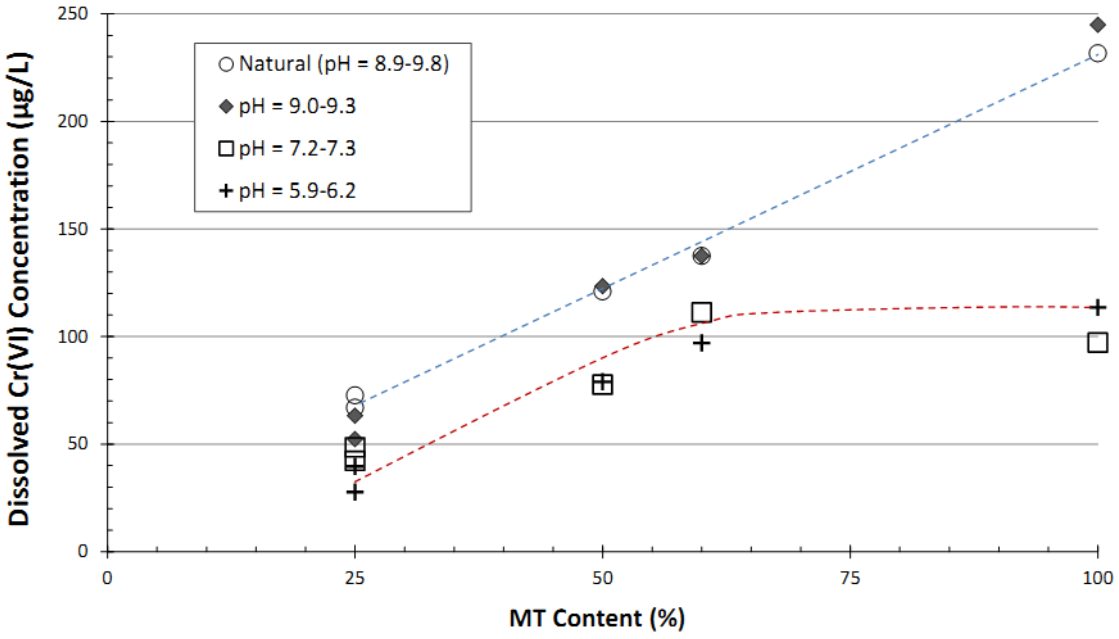

Figure 5. Total dissolved Cr concentrations from WLTs for MT-containing mixtures versus MT content (%) in the mixtures by weight. MTBS25, CPMT25, MT50, MT60 and MT100 from WLTs were grouped as unbuffered samples with natural pH values; buffered samples at pH ~6; buffered samples at pH ~6; and buffered samples at pH ~9. MTBS25 and CPMT25 were treated as samples with 25% MT content.

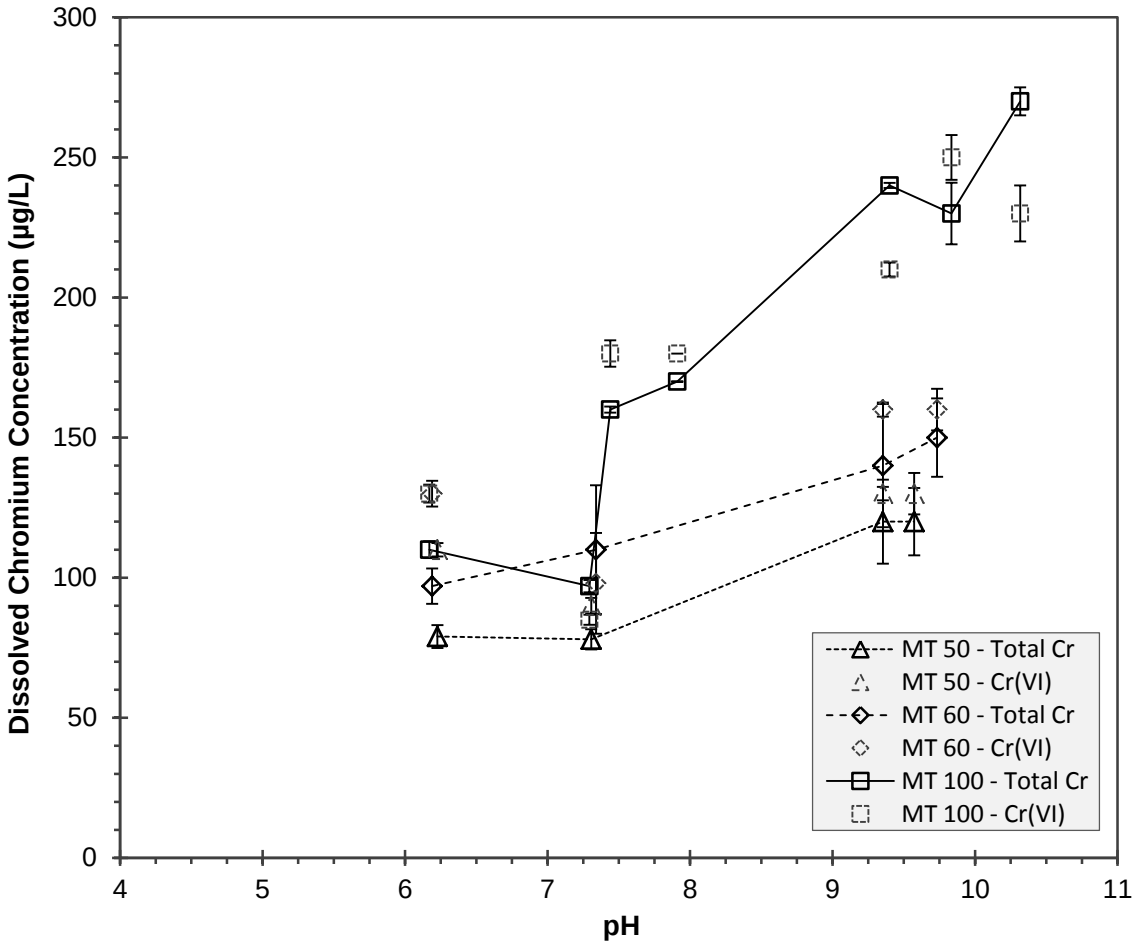

Figure 6. Dissolved total and hexavalent chromium concentrations (µg/L) from WLTs for MT100 and MT/Soil mixtures. Error bars represent the standard deviation of triplicate samples. Concentrations below detection limit (0.4 µg/L) are plotted as ½ of the detection limit.

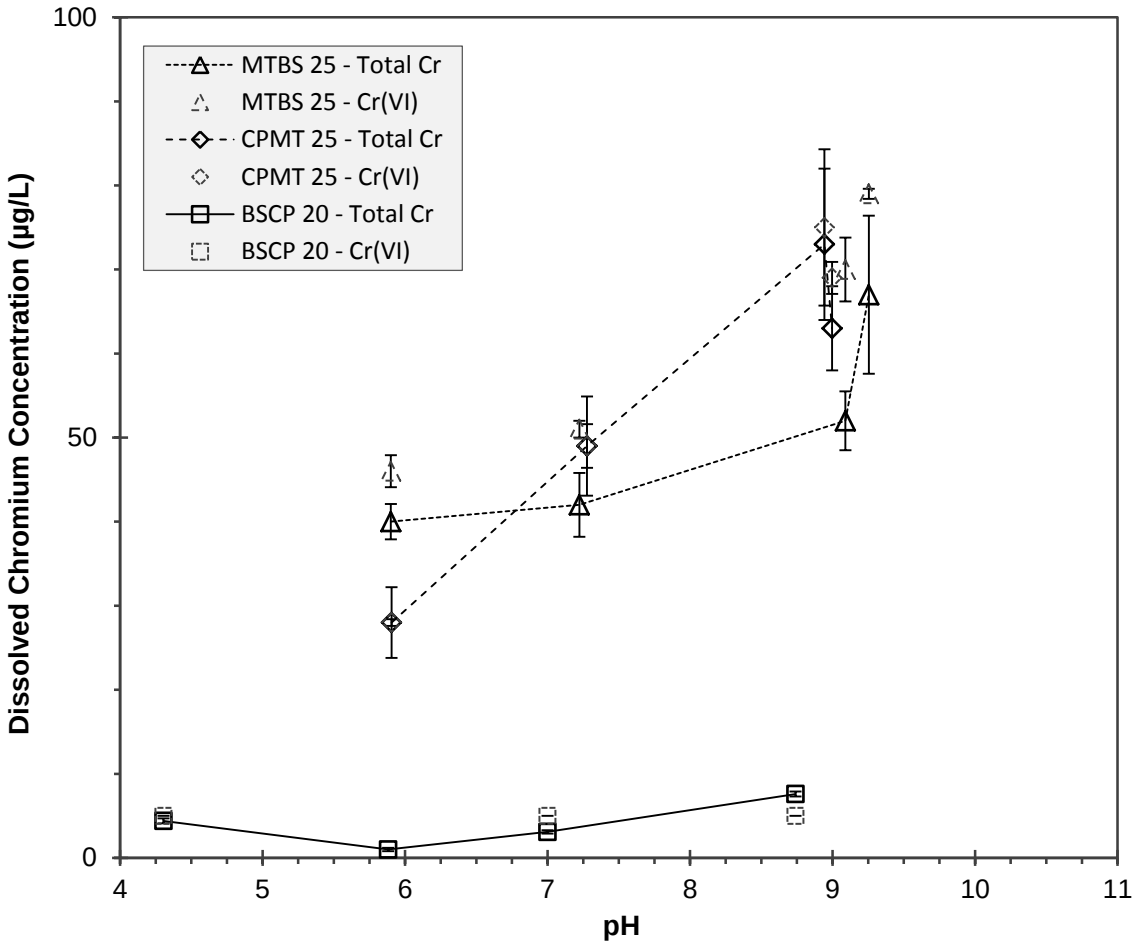

Figure 7. Dissolved total and hexavalent chromium concentrations (µg/L) from WLTs for MTBS25, CPMT25 and BSCP25 mixtures. Error bars represent the standard deviation of triplicate samples. Concentrations below detection limit (0.4 µg/L) are plotted as ½ of the detection limit.

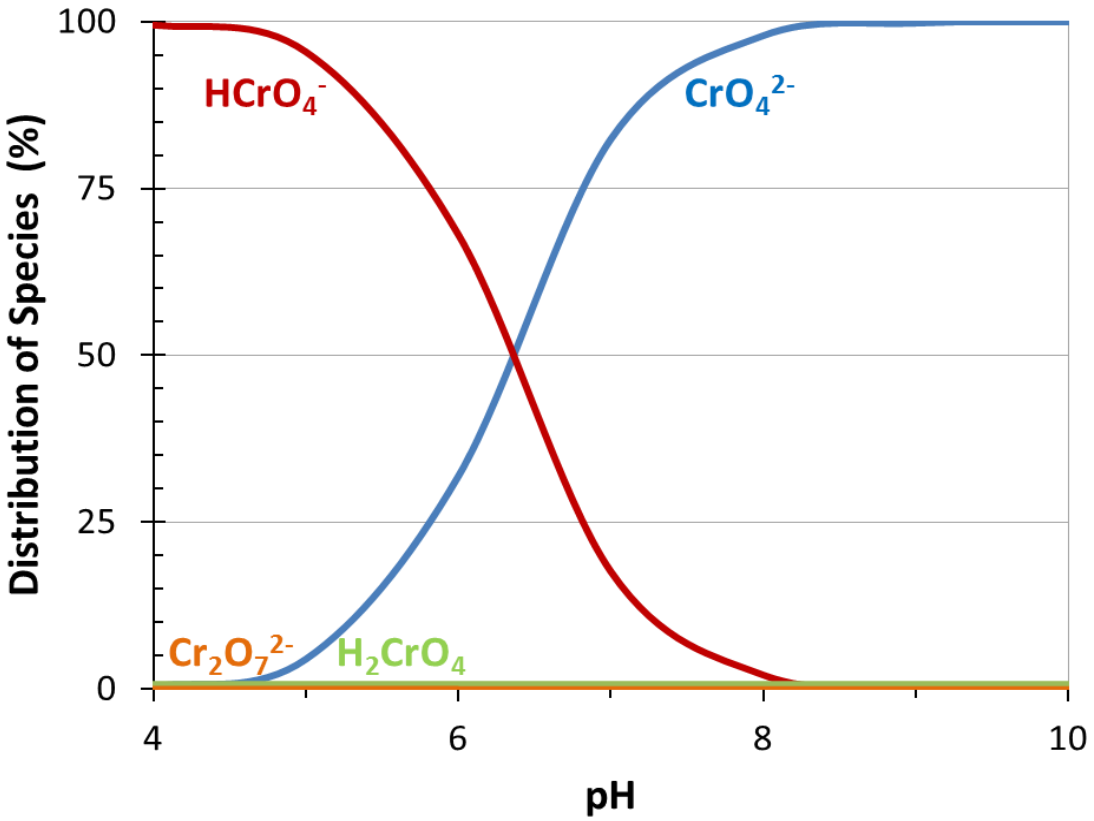

Figure 8. Effect of the pH on distribution of Cr^{VI} species. Relative distribution of species calculated by using Visual MINTEQ v3.0 beta software at fixed ionic strength of 0.02 M and a total Cr^{VI} concentration of 0.250 mg/L.

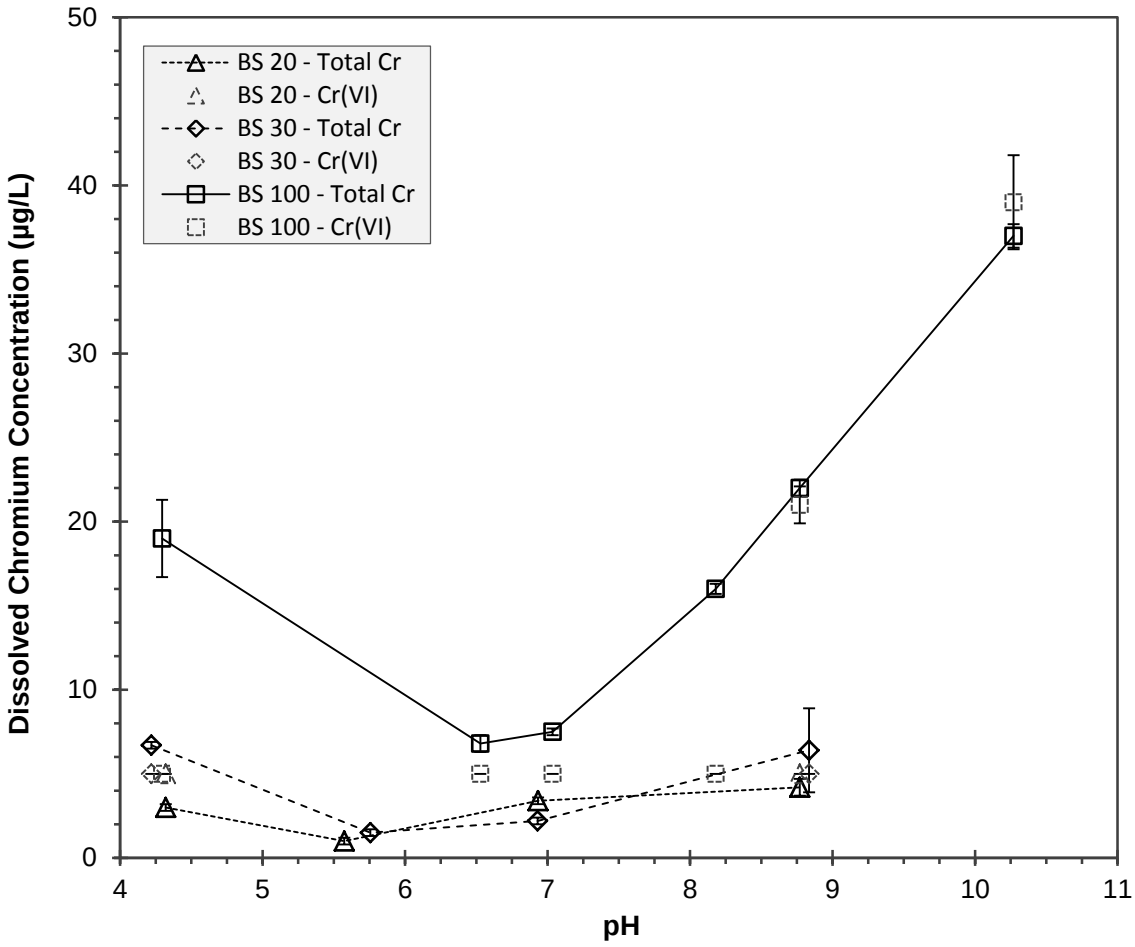

Figure 9. Dissolved total and hexavalent chromium concentrations (µg/L) from WLTs for BS100 and BS/Soil mixtures. Error bars represent the standard deviation of triplicate samples. Concentrations below detection limit (0.4 µg/L) are plotted as ½ of the detection limit.

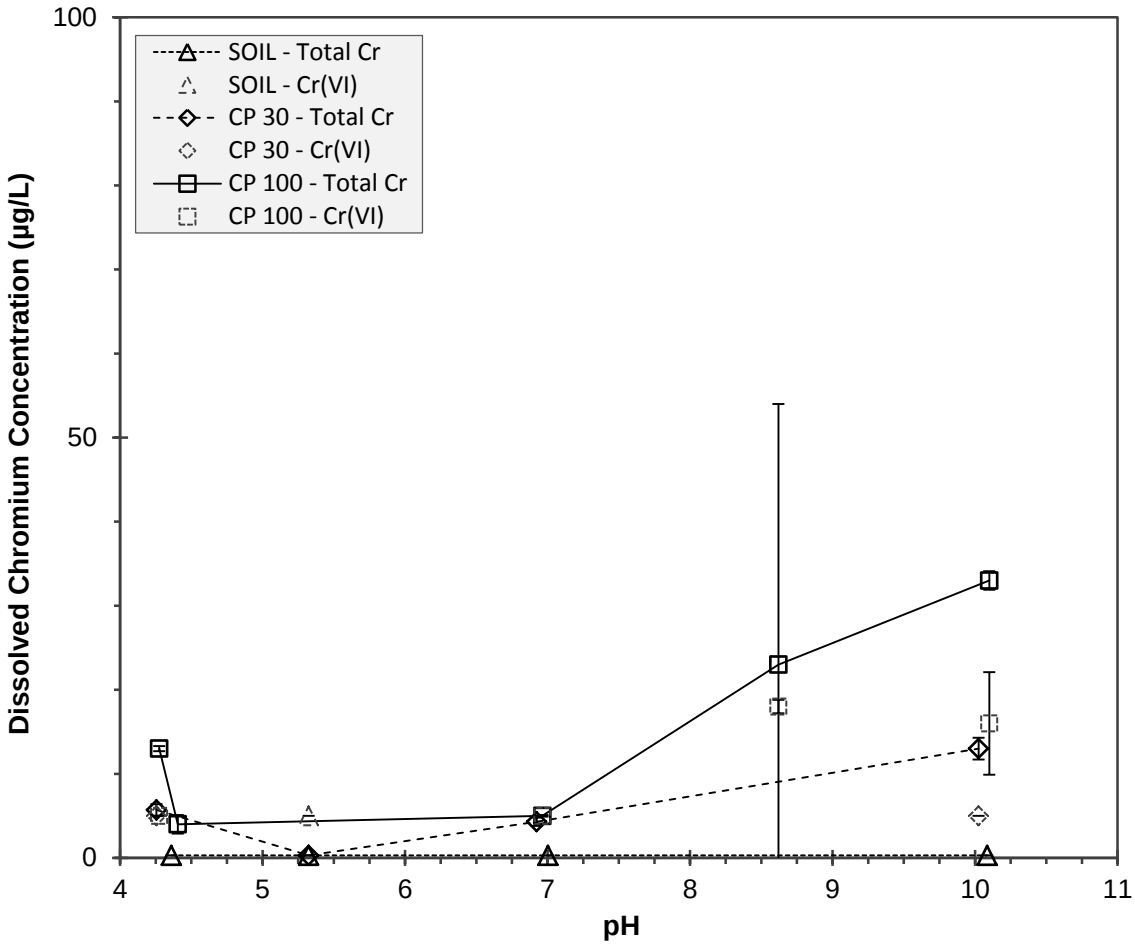

Figure 10. Dissolved total and hexavalent chromium concentrations (µg/L) from WLTs for CP100, CP30 and 100% soil. Error bars represent the standard deviation of triplicate samples. Concentrations below detection limit (0.4 µg/L) are plotted as ½ of the detection limit.

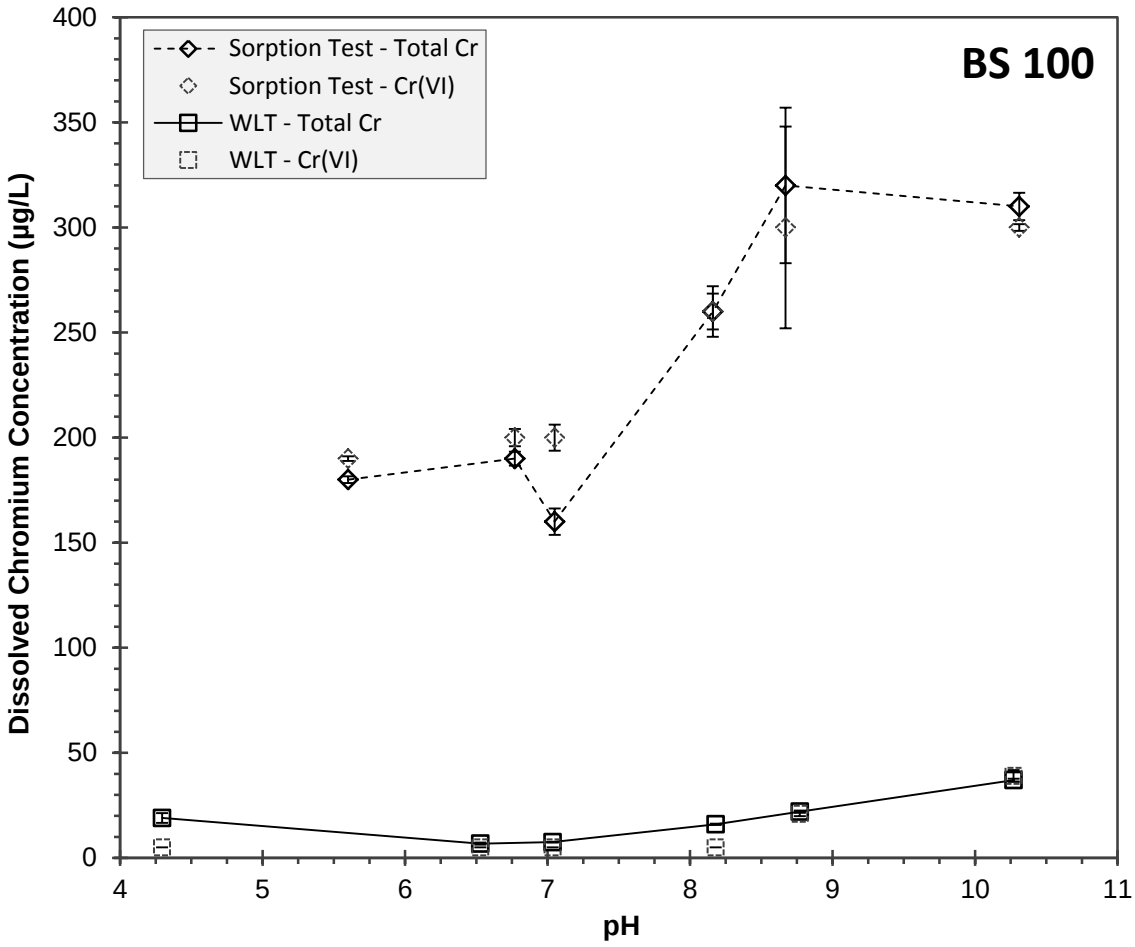

Figure 11. Residual total dissolved Cr and dissolved Cr^{VI} concentrations from sorption tests and WLTs for BS100. Sorption tests were conducted as WLTs spiked with 250 µg/L Cr^{VI}. Error bars represent the standard deviation of triplicate samples. Concentrations below detection limit (0.4 µg/L for TD Cr and 10 mg/L for Cr^{VI}) are plotted as ½ of the detection limit.

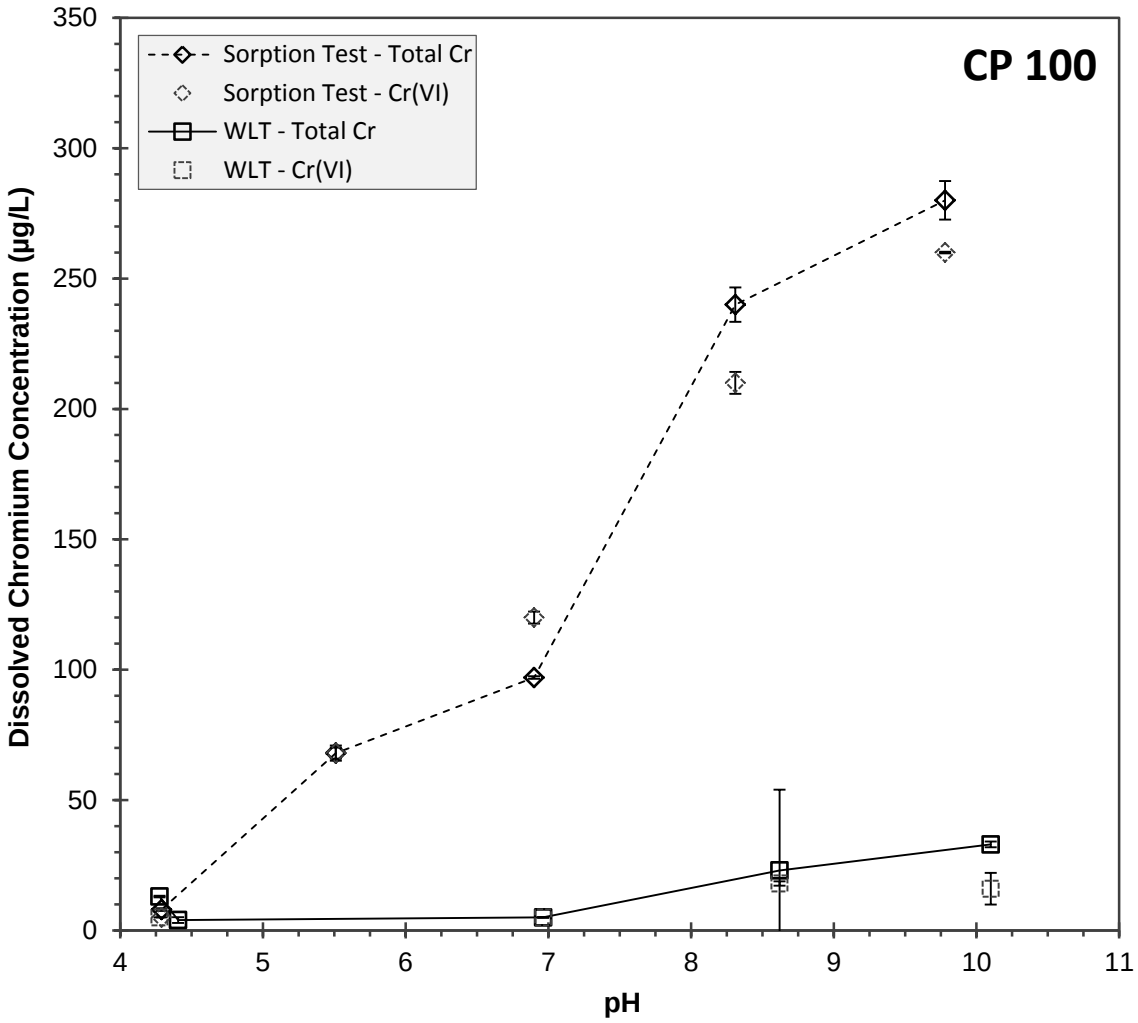

Figure 12. Residual total dissolved Cr and dissolved Cr^{VI} concentrations from sorption tests and WLTs for CP100. Sorption tests were conducted as WLTs spiked with 250 µg/L Cr^{VI}. Error bars represent the standard deviation of triplicate samples. Concentrations below detection limit (0.4 µg/L for TD Cr and 10 mg/L for Cr^{VI}) are plotted as ½ of the detection limit.

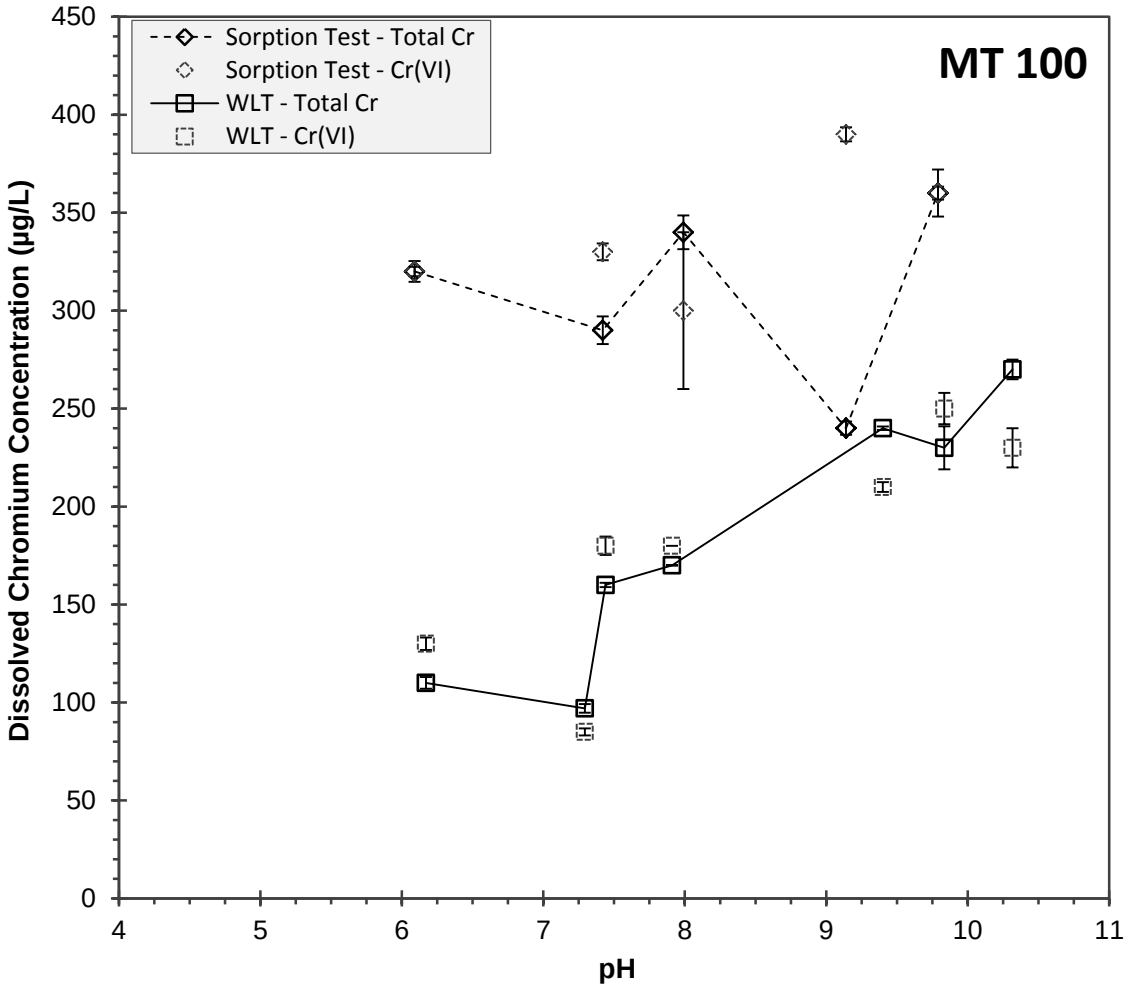

Figure 13. Residual total dissolved Cr and dissolved Cr^{VI} concentrations from sorption tests and WLTs for MT100. Sorption tests were conducted as WLTs spiked with 250 µg/L Cr^{VI}. Error bars represent the standard deviation of triplicate samples. Concentrations below detection limit (0.4 µg/L for TD Cr and 10 mg/L for Cr^{VI}) are plotted as ½ of the detection limit.

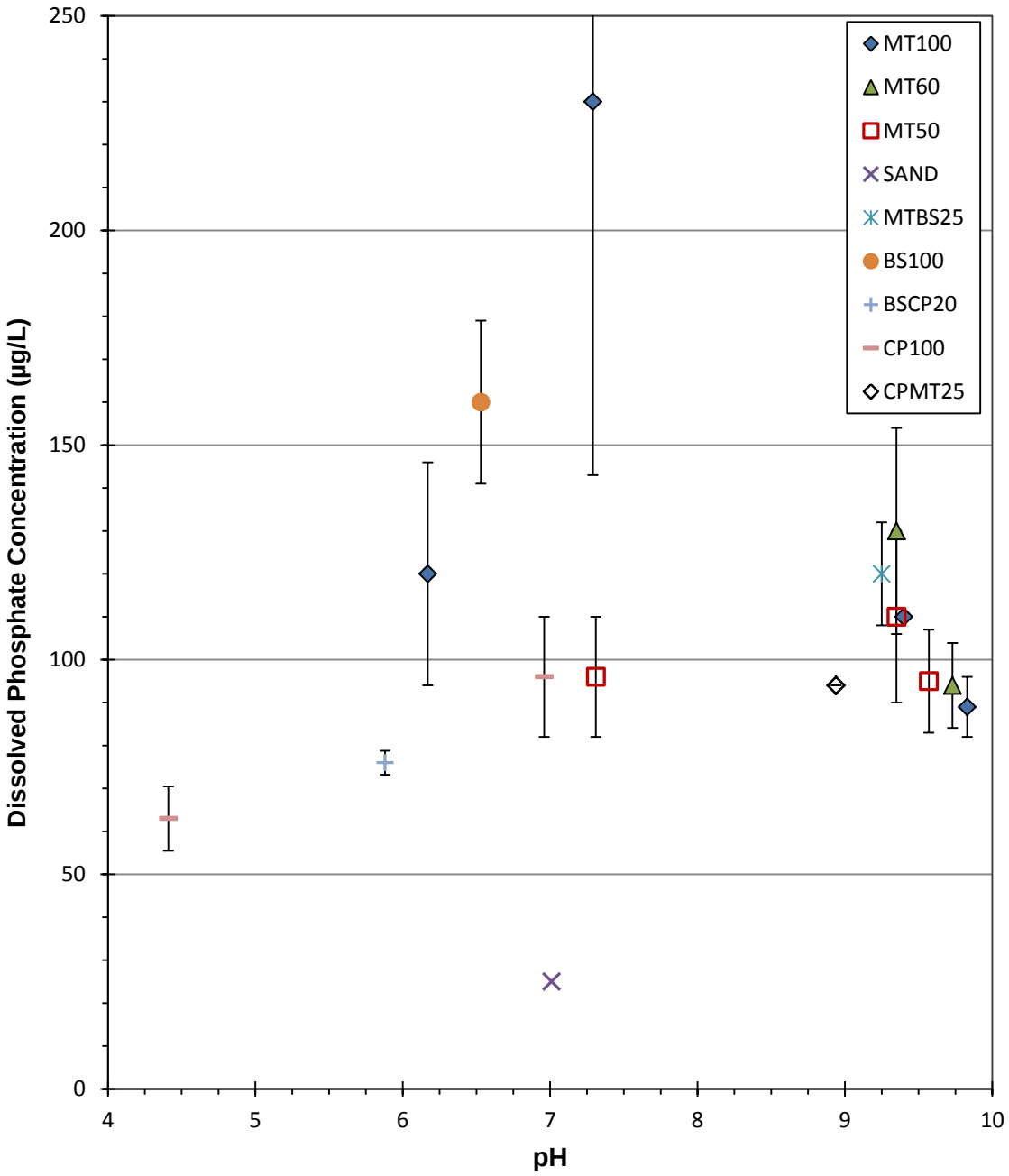

Figure 14. Dissolved phosphate concentrations from WLTs. Error bars represent the standard deviation of triplicate samples. Concentrations below detection limit (50 µg/L) are plotted as ½ of the detection limit.

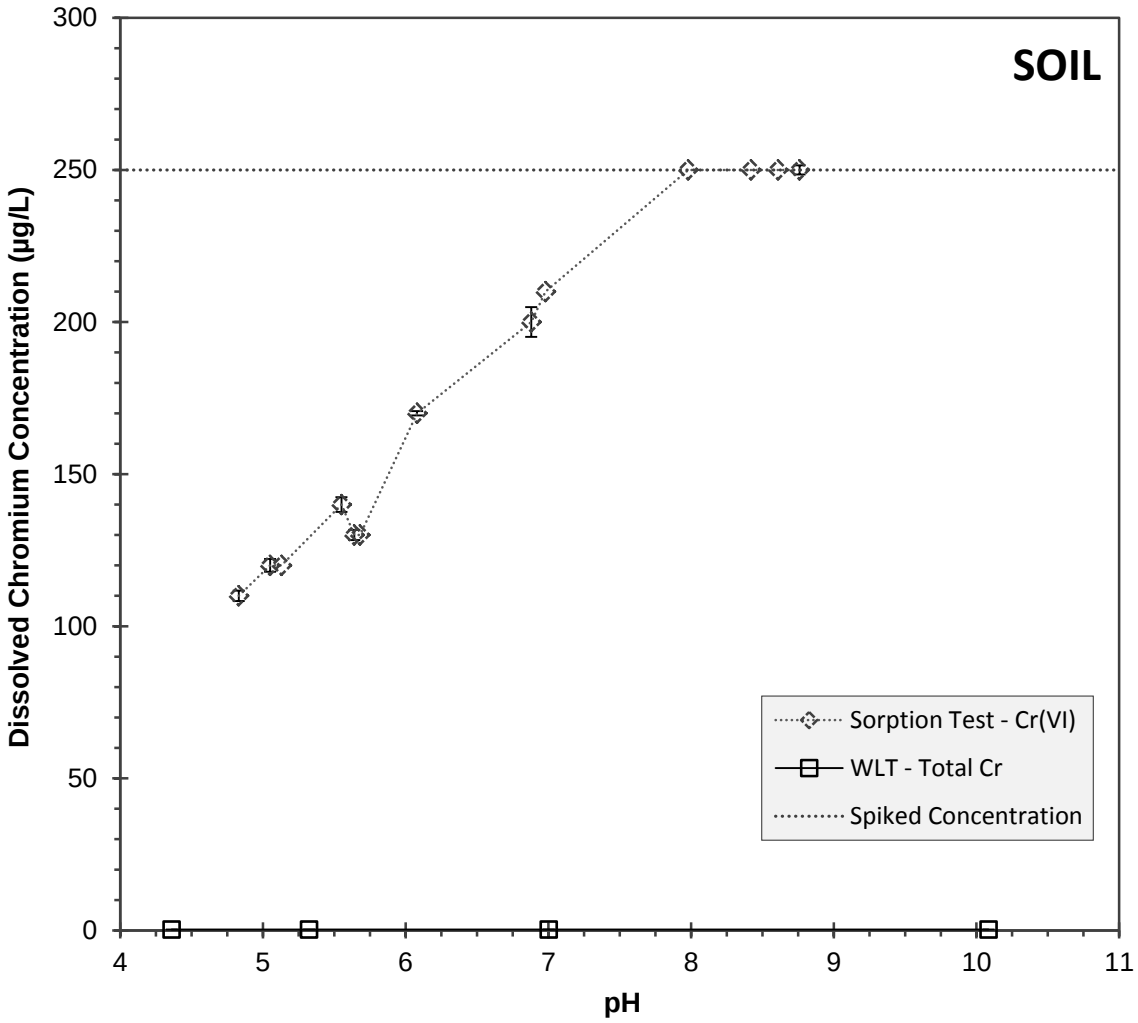

Figure 15. Residual hexavalent chromium concentrations from sorption tests for 100% soil samples, along with total dissolved Cr concentrations from WLTs. Sorption tests were conducted as WLTs spiked with 250 µg/L Cr^{VI}. Error bars represent the standard deviation of triplicate samples. Concentrations below detection limit (0.4 µg/L for TD Cr and 10 mg/L for Cr^{VI}) are plotted as ½ of the detection limit.

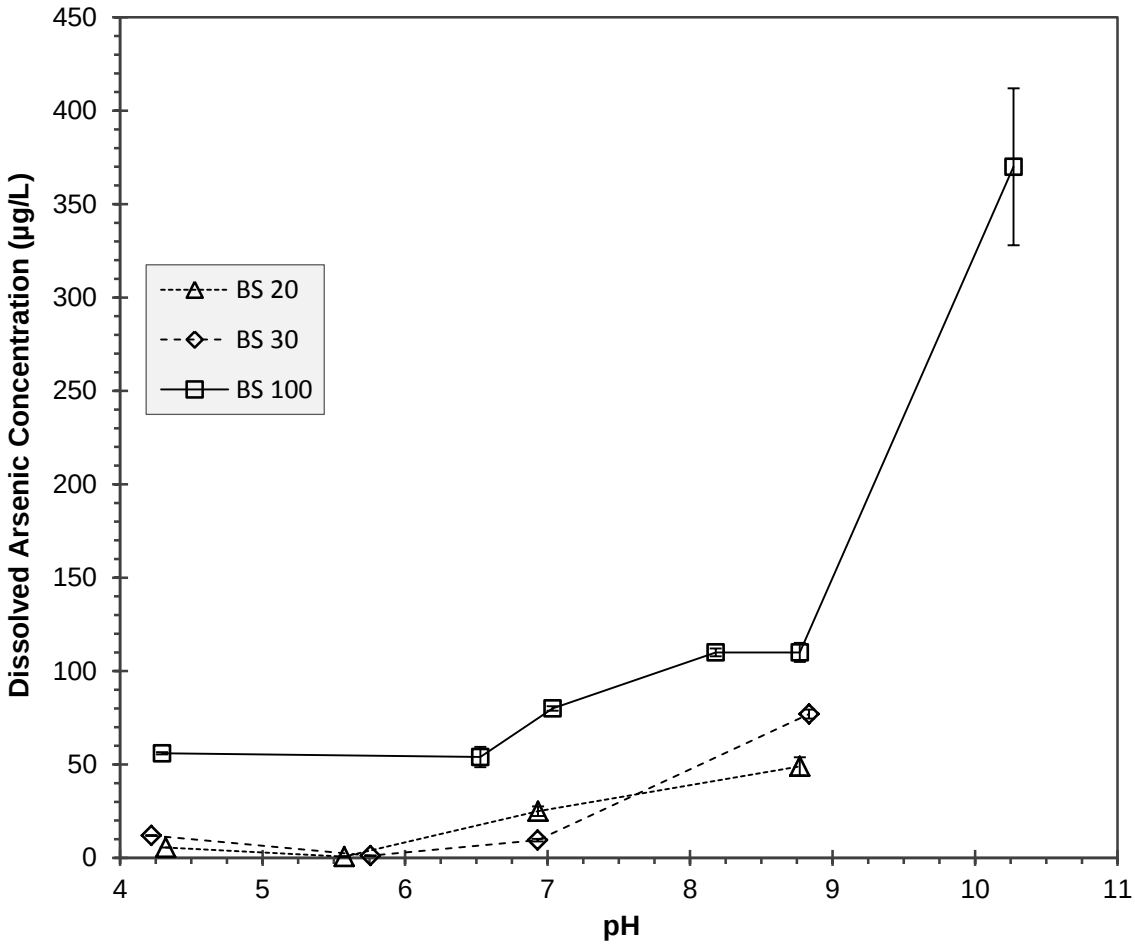

Figure 16. Dissolved arsenic concentrations (µg/L) from WLTs for BS100 and BS/Soil mixtures. Error bars represent the standard deviation of triplicate samples. Concentrations below detection limit (0.6 µg/L) are plotted as ½ of the detection limit.

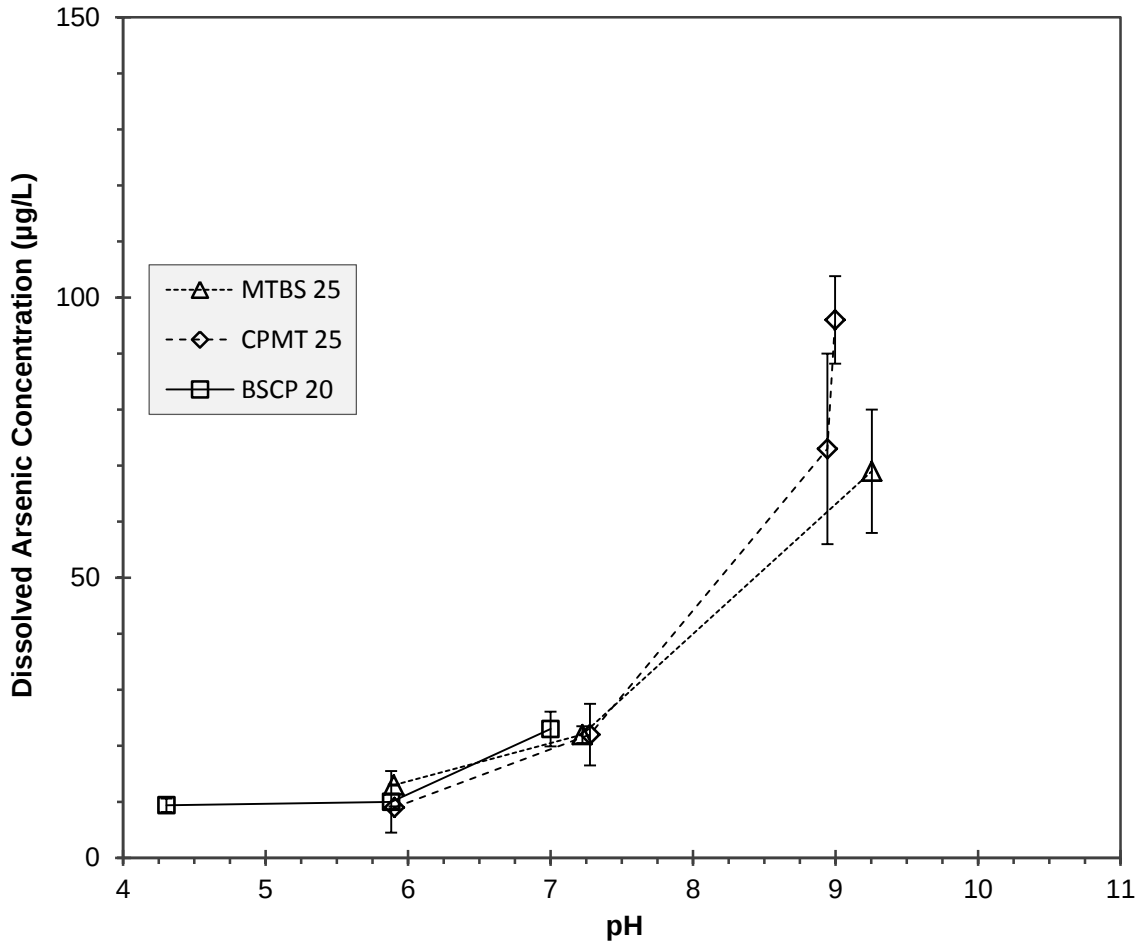

Figure 17. Dissolved arsenic concentrations (µg/L) from WLTs for MTBS25, CPMT25 and BSCP25 mixtures. Error bars represent the standard deviation of triplicate samples. Concentrations below detection limit (0.6 µg/L) are plotted as ½ of the detection limit.

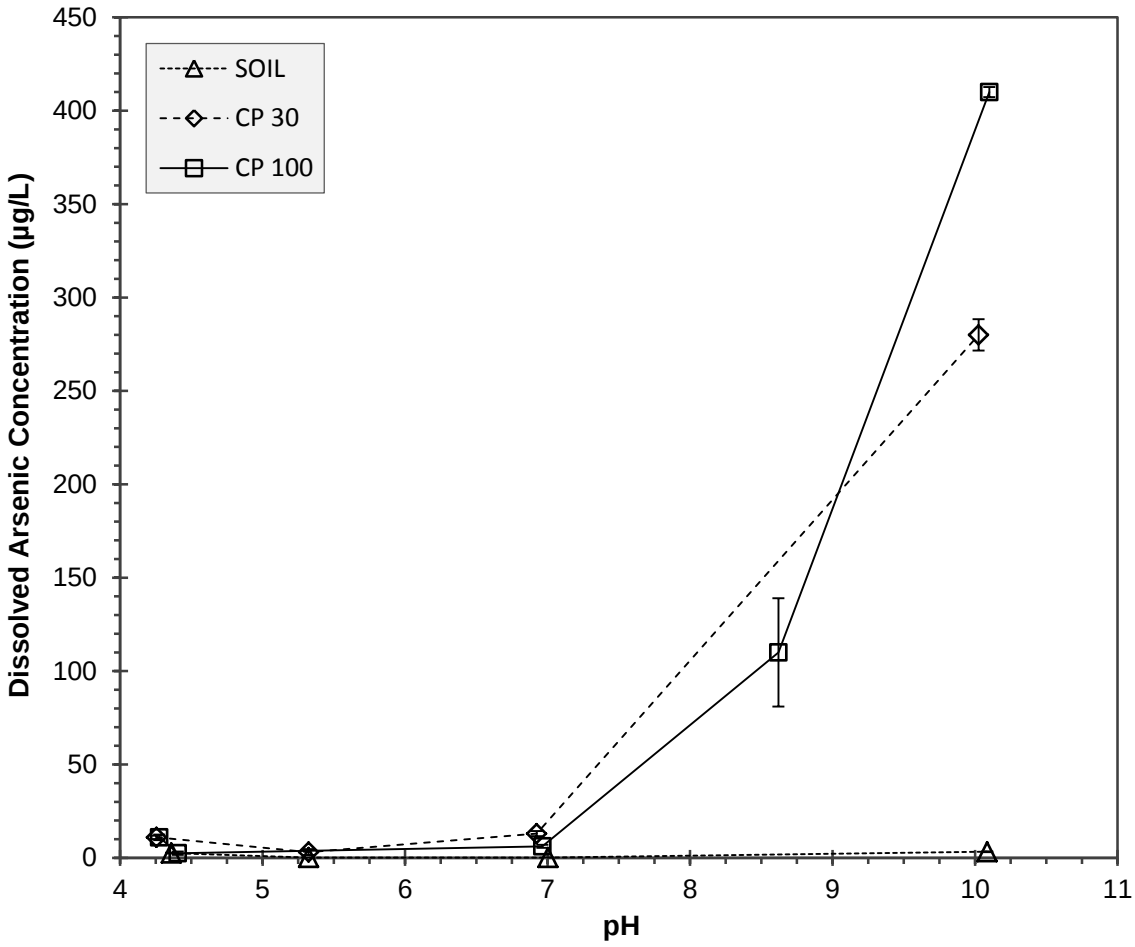

Figure 18. Dissolved arsenic concentrations (µg/L) from WLTs for CP100, CP30 and 100% soil. Error bars represent the standard deviation of triplicate samples. Concentrations below detection limit (0.6 µg/L) are plotted as ½ of the detection limit.

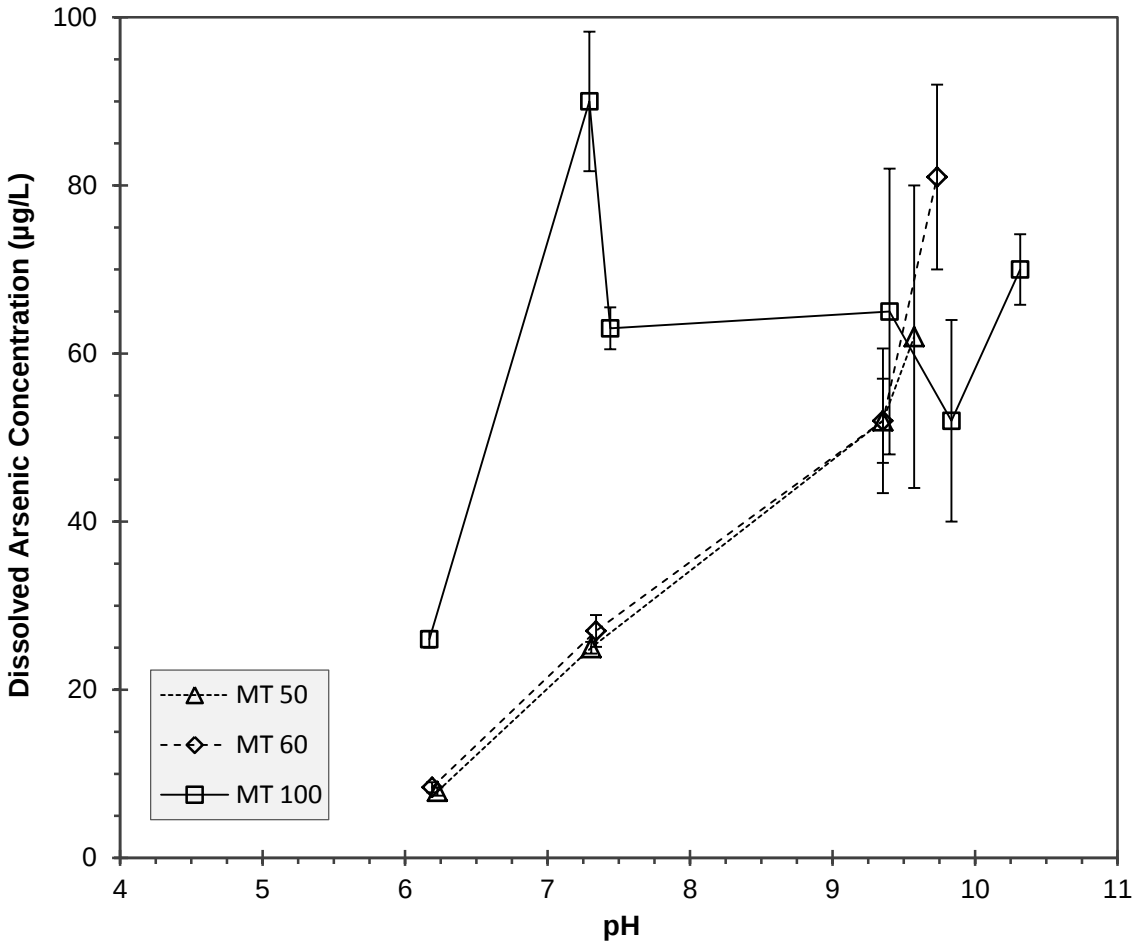

Figure 19. Dissolved arsenic concentrations (µg/L) from WLTs for MT100 and MT/Soil mixtures. Error bars represent the standard deviation of triplicate samples. Concentrations below detection limit (0.6 µg/L) are plotted as ½ of the detection limit.

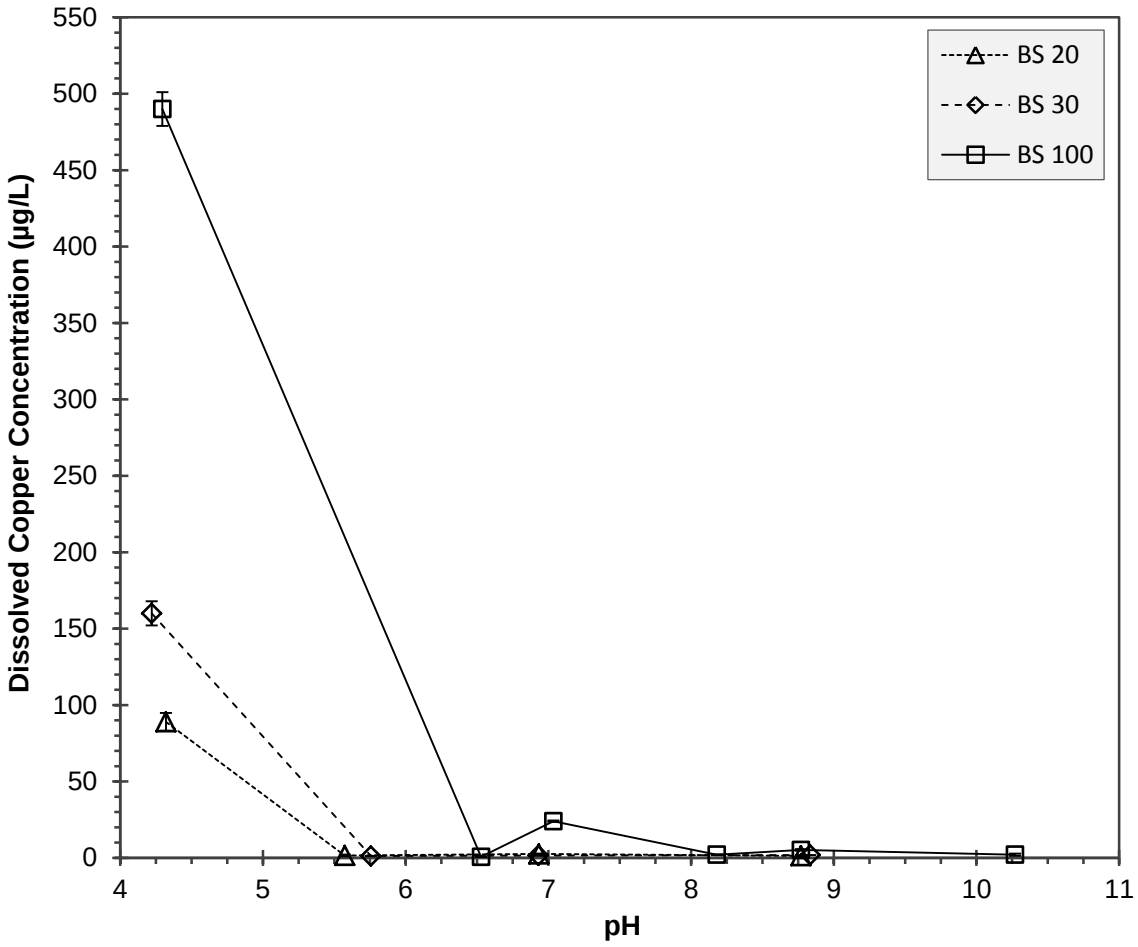

Figure 20. Dissolved copper concentrations (µg/L) from WLTs for BS100 and BS/Soil mixtures. Error bars represent the standard deviation of triplicate samples. Concentrations below detection limit (0.4 µg/L) are plotted as ½ of the detection limit.

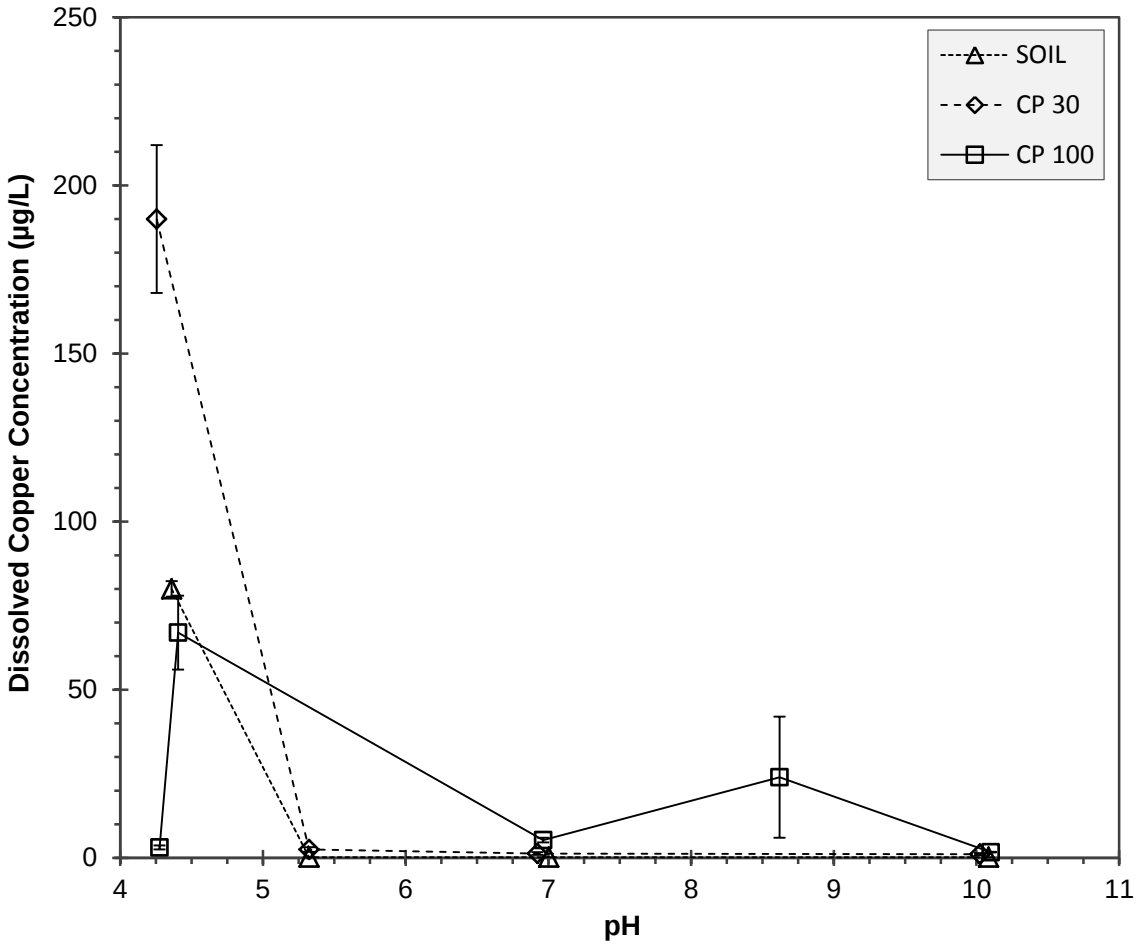

Figure 21. Dissolved copper concentrations (µg/L) from WLTs for CP100, CP30 and 100% soil. Error bars represent the standard deviation of triplicate samples. Concentrations below detection limit (0.4 µg/L) are plotted as ½ of the detection limit.

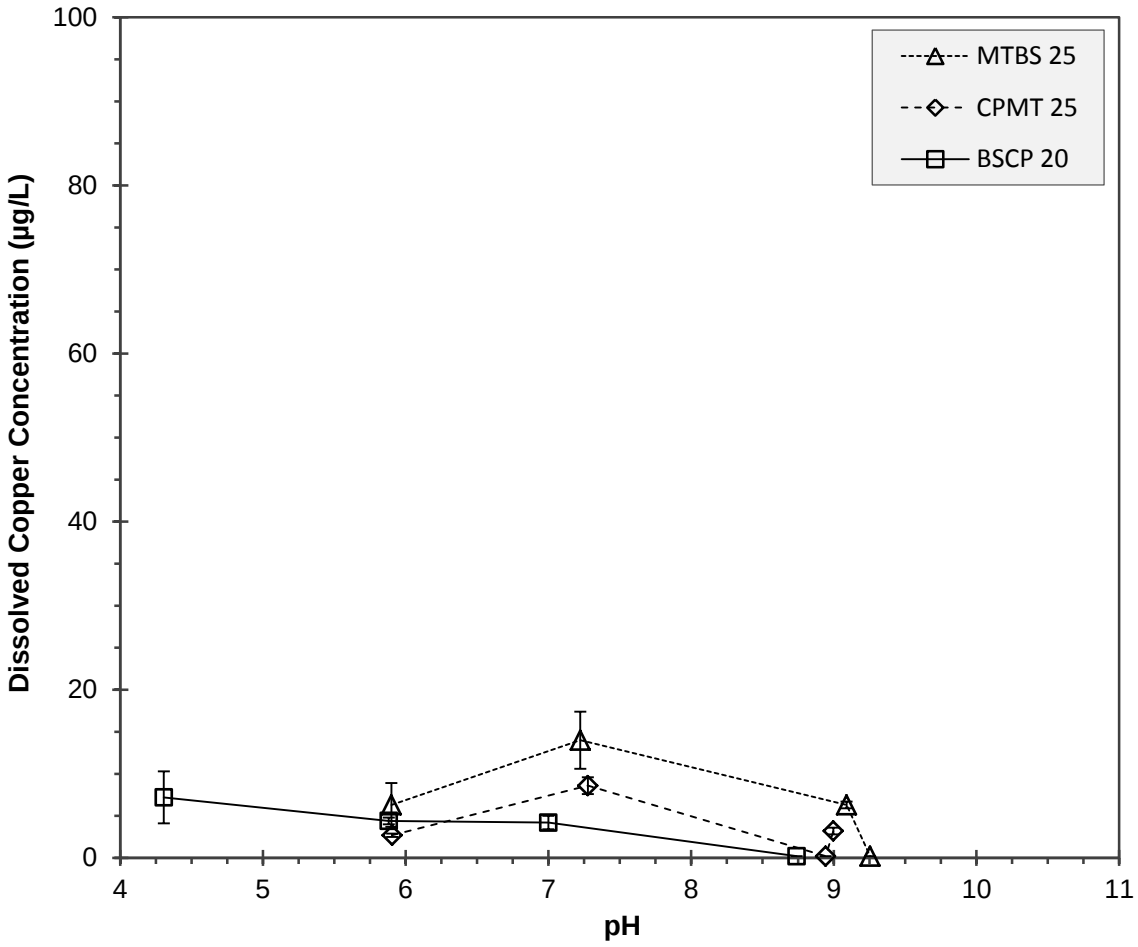

Figure 22. Dissolved copper concentrations (µg/L) from WLTs for MTBS25, CPMT25 and BSCP25 mixtures. Error bars represent the standard deviation of triplicate samples. Concentrations below detection limit (0.4 µg/L) are plotted as ½ of the detection limit.

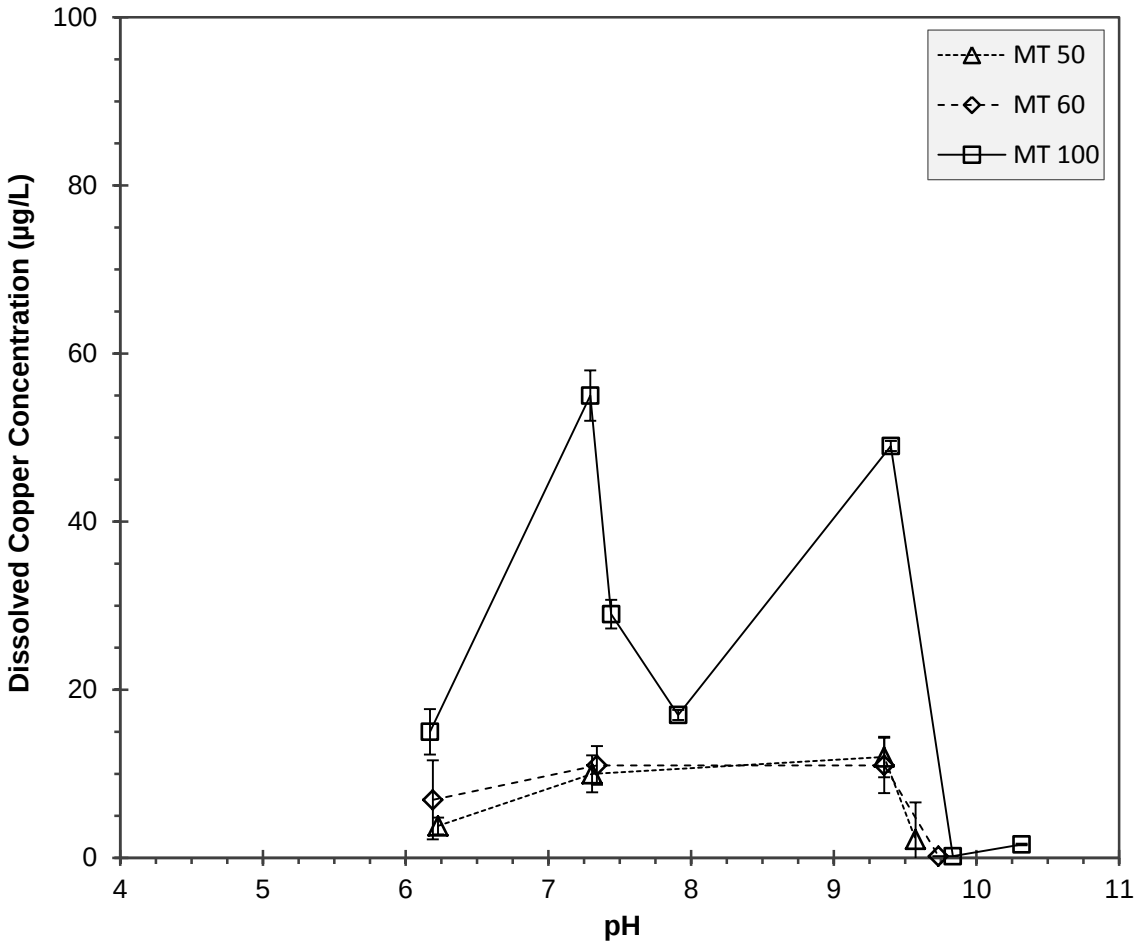

Figure 23. Dissolved copper concentrations (µg/L) from WLTs for MT100 and MT/Soil mixtures. Error bars represent the standard deviation of triplicate samples. Concentrations below detection limit (0.4 µg/L) are plotted as ½ of the detection limit.

REFERENCES

AACA (2011). Revised 2009 Coal Combustion Product (CCP) Production and Use Survey Report. The American Coal Ash Association (AACA), Aurora, CO, USA, 11.5.2011.

Ahmaruzzaman, M. (2010). A review on the utilization of fly ash. *Progress in Energy and Combustion Science, 36*, 327–363.

Al-Abed, S. R., Hageman, P. L., Jegadeesan, G., N.Madhavan, and Allen, D. (2006). Comparative Evaluation of Short-term Leach Tests for Heavy Metal Release from Mineral Processing Waste. *Science of the Total Environment*, 364, 14 – 23.

APHA (1995). Standard methods, 19th Edition, American Public Health Association, Washington, DC.

Apul, D. S., Gardner, K. H., and Eighmy, T. T. (2005). Simultaneous Application of Dissolution/Precipitation and Surface Complexation/Surface Precipitation Modeling to Contaminant Leaching. *Environ. Sci. Technol., 39*, 5736-5741.

Baba, A., and Kaya, A. (2004). Leaching characteristics of solid wastes from thermal power plants of western Turkey and comparison of toxicity methodologies. *Journal of Environmental Management, 73*, 199–207.

Baba, A., Gurda, G., and Şengünalp, F. (2010). Leaching characteristics of fl y ash from fl uidized bed combustion thermal power plant: Case study: Çan (Çanakkale-Turkey). *Fuel Processing Technology*, 91, 1073 –1080.

Bartlett, R., and James, B. (1979). Behavior of Chromium in Soils: III. Oxidation. *J. Environ. Qual., 8* (1), 31-35.

Becker, J. (2010). Evaluation of Leaching Protocols for The Testing of Coal Combustion Byproducts. MS Thesis, University of Maryland, MD, College Park.

Benjamin, M. M. (1983). Adsorption and Surface Precipitation of Metals on Amorphous Iron Oxyhydroxide. *Environ. Sci. Technol., 17*, 686-692.

Bin-Shafique, M. S., Benson, C. H., and Edil, T. B. (2002). *Leaching of Heavy Metals from Fly Ash Stabilized Soils Used In Highway Pavements.* University of Wisconsin - Madison. Madison, WI: Geo Engineering Program.

Bin-Shafique, S., Benson, C. H., Edil, T. B., and Hwang, K. (2006). Leachate Concentrations from Water Leach and Column Leach Tests on Fly Ash-Stabilized Soils. *Environmental Engineering Science, 23* (1).

Bothe, J. V., and Brown, P. W. (1999). Arsenic Immobilization by Calcium Arsenate Formation. *Environ. Sci. Technol., 33* (21), 3806–3811.

BP (2011). BP Statistical Review of World Energy, BP Global, 2011. <www.bp.com>

Coughlin, B. R., and Stone, A. T. (1995). Nonreversible Adsorption of Divalent Metal Ions (Mn^{II}, Co^{II}, Ni^{II}, Cu^{II}, and Pb^{II}) onto Goethite: Effects of Acidification, Fe^{II} Addition, and Picolinic Acid Addition. *Environ. Sci. Technol., 29*, 2445-2455 .

Çetin, B. (2009). Stabilization of recycled base materials with high carbon fly ash. *M.S. Thesis.* Civil and Environmental Engineering Dept., University of Maryland at College Park.

Çetin, B. (2010). Leaching of Heavy Metals from High Carbon Fly Ash Mixed Soils. *Ph.D. Dissertation Proposal*. Civil and Environmental Engineering Dept., University of Maryland at College Park.

Çetin, B., Aydilek, A. H., and Güney, Y. (2012). Leaching of trace metals from high carbon fly ash stabilized highway base layers. *Resources, Conservation and Recycling* (58), 8– 17.

Çetin, B., Aydilek, A. H., and Güney, Y. (2010). Stabilization of recycled base materials with high carbon fly ash. *Resources, Conservation and Recycling* (54), 878–892.

Dudas, M. J. (1981). Long-Term Leachability of Selected Elements from Fly Ash. *Environmental Science and Technology, 15* (7), 840-843.

Dudas, M. J., and Warren, C. J. (1987). Submicroscopic model of fly ash particles. *Geoderma, 40* (1-2), 101-114.

EIA. (2011,). Electric Power Annual 2009. Washington DC, USA: U.S. Energy Information Administration (EIA), April, 2010.

Evans, L. J. (1989). Chemistry of Metal Retention by Soils. *Environ. Sci. Technol., 23* (9), 1046-1056.

Fruchter, J. S., Rai, D., and Zachara, J. M. (1990). Identification of Solubility-Controlling Solid Phases in a Large Fly Ash Field Lysimeter . *Environ. Sci. Technol., 24* (8), 1173-1179 .

Gao, P., Chen, X., Shen, F., and Chen, G. (2005). Removal of chromium(VI) from wastewater by combined electrocoagulation–electroflotation without a filter. *Separation and Purification Technology, 43*, 117–123.

Gitari, W. M., Petrik, L. F., Etchebers, O., Key, D. L., and Okujeni, C. (2008). Utilization of fly ash for treatment of coal mines wastewater: Solubility controls on major inorganic contaminants. *Fuel, 87*, 2450–2462.

Goodarzi, F., and Huggins, F. E. (2005). Speciation of Arsenic in Feed Coals and Their Ash Byproducts from Canadian Power Plants Burning Sub-bituminous and Bituminous Coals. *Energy and Fuels, 19* (3), 905-915.

Goodarzi, F., Huggins, F. E., and Sanei, H. (2008). Assessment of elements, speciation of As, Cr, Ni and emitted Hg for a Canadian power plant burning bituminous coal. *International Journal of Coal Geology, 74*, 1–12.

Hèquet, V., Ricou, P., Lecuyer, I., and Cloirec, P. L. (2001). Removal of Cu2+ and Zn2+ in aqueous solutions by sorption onto mixed fly ash. *Fuel, 80*, 851-856.

Hill, R. L., Sarkar, S. L., Rathbone, R. F. and Hower, J. C. (1997). An examination of fly ash carbon and its interactions with Air entraining agent. *Cement and Concrete Research, 27 (2)*, 193-204.

Hohl, H., Sigg, L., and Stumm, W. (1980). Characterization of Surface Chemical. In M. E. Kavanaugh, *Particulates in Water.*

Hower, J. C., Rathbone, R. F., Robl, T. L., Thomas, G. A., Haeberlin, B. O., and Trimble, A. S. (1998). Case study of the conversion of tangential- and wall-fired units to low-NOx combustion: Impact on fly ash quality. *Waste Management, 17* (4), 219-229.

Hsia, T. H., Lo, S. L., Lin, C. F., and Lee, D. Y. (1993). Chemical and spectroscopic evidence for specific adsorption of chromate on hydrous iron oxide. *Chemosphere, 26* (10), 1897-1904.

Huggins, F. E., Najih, M., and Huffman, G. P. (1999). Direct speciation of chromium in coal combustion by-products by X-ray absorption fine-structure spectroscopy. *Fuel, 78* (2), 233-242.

Huggins, F. E., Senior, C. L., Chu, P., Ladwig, K., and Huffman, G. P. (2007). Selenium and Arsenic Speciation in Fly Ash from Full-Scale Coal-Burning Utility Plants. *Environ. Sci. Technol., 41* (9), 3284–3289.

Izquierdoa, M., and Querol, X. (2011). Leaching behaviour of elements from coal combustion fly ash: An overview. *Geology, International Journal of Coal* , In Press, Corrected Proof.

Jackson, B. P., and Miller, W. P. (1998). Arsenic and selenium speciation in coal fly ash extracts by ion chromatography-inductively coupled plasma mass spectrometry. *J. Anal. At. Spectrom., 13*, 1107–1112.

Jegadeesan, G., Al-Abed S., Pinto, P. (2008). Influence of trace metal distribution on its leachability from coal fly ash. *Fuel. 87,* 1887-1893.

Jo, H., Minb, S., Lee, T., Ahna, H., Lee, S., Honga, J. (2008). Environmental feasibility of using coal ash as a fill material to raise the ground level. *J. Hazard Mater. 154,* 933-945.

Keefer, R. F., and Sajwan, K. S. (1993). *Trace Elements in Coal and Coal Combustion Residues.* Lewis Publishers.

Kim, A. G. (2006). The effect of alkalinity of Class F PC fly ash on metal release . *Fuel , 85*, 1403–1410.

Komonweeraket, K., Benson, C. H., Edil T. B. and Bleam, W. F. (2010). Mechanisms controlling leaching of heavy metals from soil stabilized with fly ash. Geo Engineering Report No. 02-14; 2010. Madison, WI: Geo Engineering Program, University of Wisconsin-Madison.

Kosson, D. S., van der Sloot, H. A., Sanchez, F., and Garrabrants, A. C. (2002). An integrated framework for evaluating leaching in waste management and utilization of secondary materials. *Environmental Engineering Science, 19* (3), 159-204.

Lin, C. J., and Chang, J. E. (2001). Effect of fly ash characteristics on the removal of Cu(II) from aqueous solution. *Chemosphere, 44* (5), 1185.

Lindon, S. K. (2001). *The properties and use of coal fly ash: A valuable industrial by-product.* U.K.: Tomas Telford Ltd.

Loeppert, R. H., Jain, A., El-Haleem, M. A., and Biswas, B. K. (2002). Quantity and Speciation of Arsenic in Soils by Chemical Extraction. In Y. Cai, and O. C. Braids, *Biogeochemistry of Environmentally Important Trace Elements* (Vol. 835, pp. 42–56). ACS Symposium Series.

McKeague, J. A., and Day, J. H. (1966). Dithionite- and oxalate-extractable Fe and Al as aids in differentiating various classes of soils. *Can. J. Soil Sci. , 46*.

Mesuere, K., and Fish, W. (1992). Chromate and Oxalate Adsorption on Goethite. 2. Surface Complexatlon Modeling of Competitive Adsorption. *Envlron. Scl. Technol. , 26*, 2365-2370.

Morar, D. L. (2008). Leaching of metals from fly ash-amended permeable reactive barriers. MS Thesis, University of Maryland, MD, College Park.

Nathana, Y., Dvoracheka, M., Pelly, I., and Mimran, U. (1999). Characterization of coal fly ash from Israel. *Fuel, 78*, 205-213.

Nelson, P. F., Shah, P., Strezov, V., Halliburton, B., and Carras, J. N. (2010). Environmental impacts of coal combustion: A risk approach to assessment of emissions. *Fuel, 89*, 810–816.

PPRP (2008). *Maryland Power Plants and Environment* (Vols. CEIR-14). Maryland Power Plant Research Program (PPRP), Maryland Department of Natural Resources (DNR), DNR Publication No. 12-1142008-271, Annapolis, MD, USA.

Querol, X., Umaña, J. C., Alastuey, A., Ayora, C., Lopez-Soler, A., and Plana, F. (2001). Extraction of soluble major and trace elements from fly ash in open and closed leaching systems. *Fuel, 80*, 801-813.

Querol, X., Juan, R., Lopez-Soler, A., Fernandez-Turiel, J. L., and Ruiz, C. R. (1996). Mobility of trace elements from coal and combustion wastes. *Fuel, 75* (7), 821-838.

Raven, K. P., Jain, A., and Loeppert, R. H. (1998). Arsenite and Arsenate Adsorption on Ferrihydrite: Kinetics, Equilibrium, and Adsorption Envelopes. *Environ. Sci. Technol. 1998, 32* (3), 344-349.

Reddy, K. J., Wang, L., and Gloss, S. P. (1995). Solubility and Mobility of Copper, Zinc and Lead in Acidic Environments. *Plant and Soil, 171*, 53-58.

Shah, P., Strezov, V., Prince, K., and Nelson, P. F. (2008). Speciation of As, Cr, Se and Hg under coal fired power station conditions. *Fuel, 87*, 1859–1869.

Shah, P., Strezov, V., Stevanov, C., and Nelson, P. F. (2007). Speciation of Arsenic and Selenium in Coal Combustion Products. *Energy and Fuels, 21*, 506-512.

Simòn, M., and Garcìa, I. (1999). Physico-chemical properties of the soil-saturation extracts: estimation from electrical conductivity. *Geoderma, 90*, 99–109.

Soco, E., and Kalembkiewicz, J. (2009). Investigations on Cr mobility from coal fly ash. *Fuel, 88*, 1513–1519.

Sparks, D. L. (2003). *Environmental Soil Chemistry* (2nd ed.). San Diago, California: Academic Press.

Sposito, G. (2008). *The Chemistry of Soils* (2nd ed.). New York, NY, USA: Oxford University Press.

Stollenwerk, K. (2003). Geochemical Processes Controlling Transport of Arsenic in Groundwater: A Review of Adsorption. In A. H. Welch, and K. G. Stollenwerk (Eds.), *Arsenic in Ground Water.*

Stumm, W., and Morgan, J. J. (1996). The Solid-Solution Interface. In *Aquatic Chemistry* (3rd ed. ed., pp. 517-613). New York: John Wiley and Sons.

Takeno, N. (2005). Atlas of Eh-pH Diagrams: Intercomparison of Thermo Dynamic Database. *Geological Survey of Japan Open File Report No.419*. National Institute of Advanced Industrial Science and Technology, Research Center for Deep Geological Environments.

Talbot, R. W., Anderson, M. A., and Andren, A. W. (1978). Qualitative model of heterogeneous equilibriums in a fly ash pond. *Environ. Sci. Technol., 12* (9), 1056–1062.

Theis, T. L., and Wirth, J. L. (1977). Sorptive behavior of trace metals on fly ash in aqueous systems. *Environ. Sci. Technol., 11* (12), 1096-1100.

Turner, D. R., Whitefield, M., and Dickson, A. G. (1981). The equilibrium speciation of dissolved components in freshwater and seawater at 25 C and 1 atm pressure. *Geochimica et Cosmochimica Acta* (45), 855-881.

Turner, R. R. (1981). Oxidation State of Arsenic in Coal Ash Leachate . *Environmental Science and Technology, 15* (9), 1062-1066.

Twardowska, I., and Stefaniak, S. (2006). Coal and Coal Combustion Products: Prospects for Future and Environmental Issues. In K. S. Sajwan, I. Twardowska, T. Pushon, and A. K. Alva (Eds.), *Coal Combustion Byproducts and Environmental Issues* (pp. 13-20). New York, NY, USA: Springer Science+Business Media, Inc.

USEPA (2007). *The Use of Soil Amendments for Remediation, Soil Amendments for Remediation, Revitalization, and Reuse*. U.S. Environmental Protection Agency (USEPA), Office of Superfund Remediation and Technology Innovation (OSRTI), EPA 542-R-07-013, Cincinnati, OH.

USGS (2002). *Characterization and Modes of Occurrence of Elements in Feed Coal and Fly Ash - An integrated Approach*. U.S. Geological Survey (USGS), Fact Sheet-038-02.

van der Hoek, E. E., and Comans, R. N. (1996). Modeling Arsenic and Selenium Leaching from Acidic Fly Ash by Sorption on Iron (Hydr)oxide in the Fly Ash Matrix. *Environ. Sci. Technol., 30* (2), 517–523.

van der Hoek, E. E., Bonouvrie, P. A., and Comans, R. N. (1994). Sorption of As and Se on mineral components of fly ash: relevance for leaching processes. *Applied Geochemistry, 9*, 403-412.

van der Sloot, H. A., Seignette, P., Comans, R. N., Van Zomeren, A., Dijkstra, J. J., Meeussen, H., et al. (2003). Evaluation of environmental aspects of alternative materials using an integrated approach assisted by a database/expert system. *Recycling and Reuse of Waste Materials, Proceedings of the International Symposium*, (pp. 769-789). Dundee, UK.

Wagemann, R. (1978). Some theoretical aspects of stability and solubility of inorganic arsenic in the freshwater environment. *Water Research, 12*, 139-145.

Wang, T., Wang, J., Tang, Y., Shi, H., and Ladwig, K. (2009). Leaching Characteristics of Arsenic and Selenium from Coal Fly Ash: Role of Calcium. *Energy and Fuels*, 23, 2959–2966.

Wang, W., Qin, Y., D.Song, and Wang, K. (2008). Column leaching of coal and its combustion residues, Shizuishan, China. *International Journal of Coal Geology, 75*, 81–87.

Ward, C. R., French, D., Jankowski, J., Dubikova, M., Li, Z., and Riley, K. W. (2009). Element mobility from fresh and long-stored acidic fl y ashes associated with an Australian power station. *International Journal of Coal Geology, 80*, 224–236.

WCI (2009). The Coal Resource: A Comprehensive Overview of Coal, UK: World Coal Institute, March 6, 2009. <www.worldcoal.org>

Yoon, S., Balunaini, U., Yildirim, Z. I., Prezzi, M., and Siddiki, N. (2009). Construction of embankment with fly and bottom ash mixture, Field performance study. *J.Mat. in Civ. Engrg., 21* (6), 271–278.

Yu, T. R. (1997). *Chemistry of Variable Charge Soils.* Oxford University Press, New York, NY.

Zachara, J. A., Girvln, D. C., Schmidt, R. L., and Resch, C. T. (1987). Chromate Adsorption on Amorphous Iron Oxyhydroxide in the Presence of Major Groundwater Ions. *Environ. Sci. Technol., 21*, 589-594 .

Zhu, C. (2002). Estimation of surface precipitation constants for sorption of divalent metals onto hydrous ferric oxide and calcite. *Chemical Geology* (188), 23–32.